

# Searching for Gravitational Waves associated with Flaring galactic Magnetars

Kara Merfeld  
University of Oregon  
28 April, 2023

Dissertation Committee:

Dr. Raymond Frey (Advisor)

Dr. Ben Farr (Chair)

Dr. Carol Paty

Dr. Robert Schofield

Dr. Laura Jeanty

# Structure of Talk:

1. Introduction to gravitational waves and the LIGO observatories
2. Presentation of two of my DetChar and commissioning projects when I was an LSC Fellow, 2018-2019
3. Magnetars and the O3 x-ray burst GW follow-up search
4. The GW search over Fast Radio Bursts in O3a
5. Preparations for O4: a stacked analysis

# General Relativity:

In 1915, Einstein came up with General Relativity, which describes perturbations to the flat space metric as propagating waves:

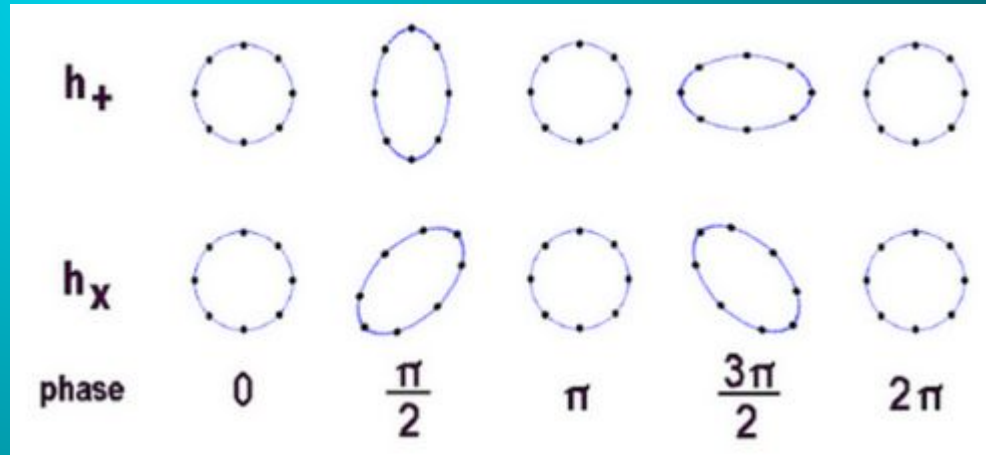
$$-\square \bar{h}_{\alpha\beta} = \frac{16\pi G}{c^4} \tau_{\alpha\beta}$$

For a plane-wave traveling in the z-direction:

$$h(t, z) = \begin{pmatrix} 0 & 0 & 0 & 0 \\ 0 & h_+ & h_x & 0 \\ 0 & h_x & -h_+ & 0 \\ 0 & 0 & 0 & 0 \end{pmatrix} e^{i\omega(z-ct)}$$

$$\frac{\delta L_x}{L_x} = +\frac{1}{2} h_+ \sin(\omega t) \quad \frac{\delta L_y}{L_y} = -\frac{1}{2} h_+ \sin(\omega t)$$

The time-varying effects of a gravitational-waves on a ring of point particles:



# Gravitational-wave observatories:

LIGO Livingston (LA)



LIGO Hanford (WA)



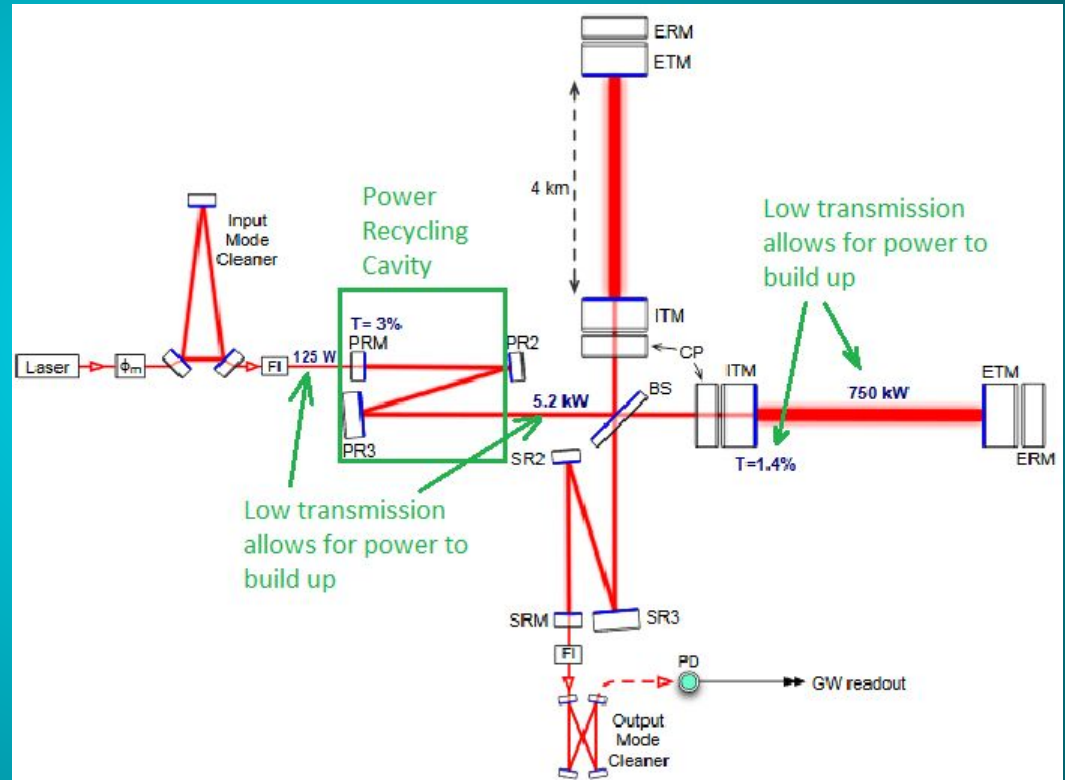
Virgo Observatory,  
Pisa, Italy





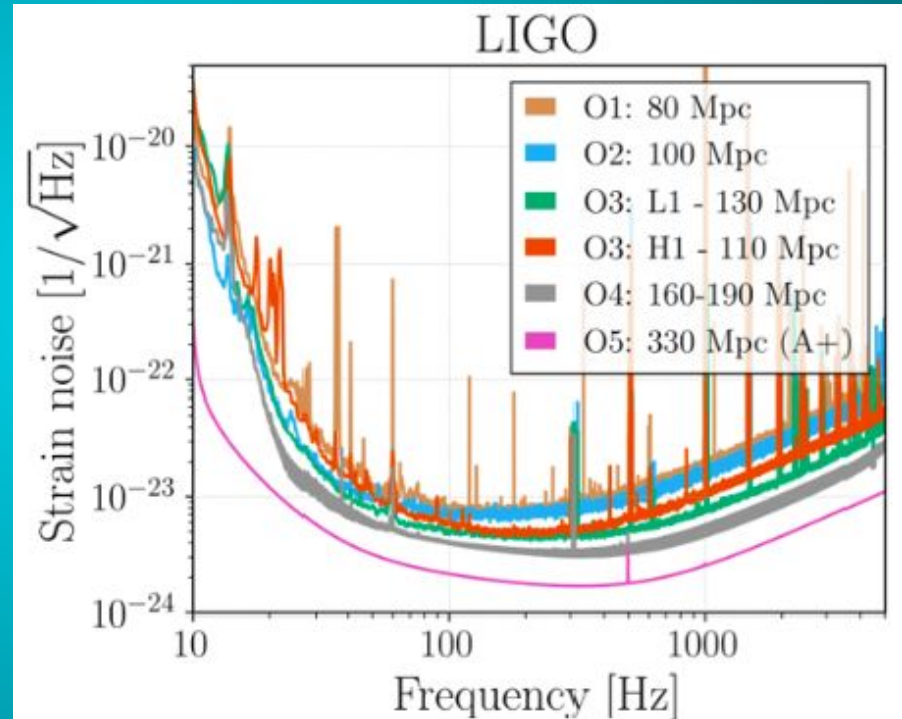
# LIGO optical setup

- Observatories combine a Michelson interferometer with two 4km Fabry-Perot cavities
- Measures the difference in arm length (DARM) by measuring the phase difference.
- Power is built up in stages before it reaches the Fabry-Perot cavities.



# LIGO sensitivity

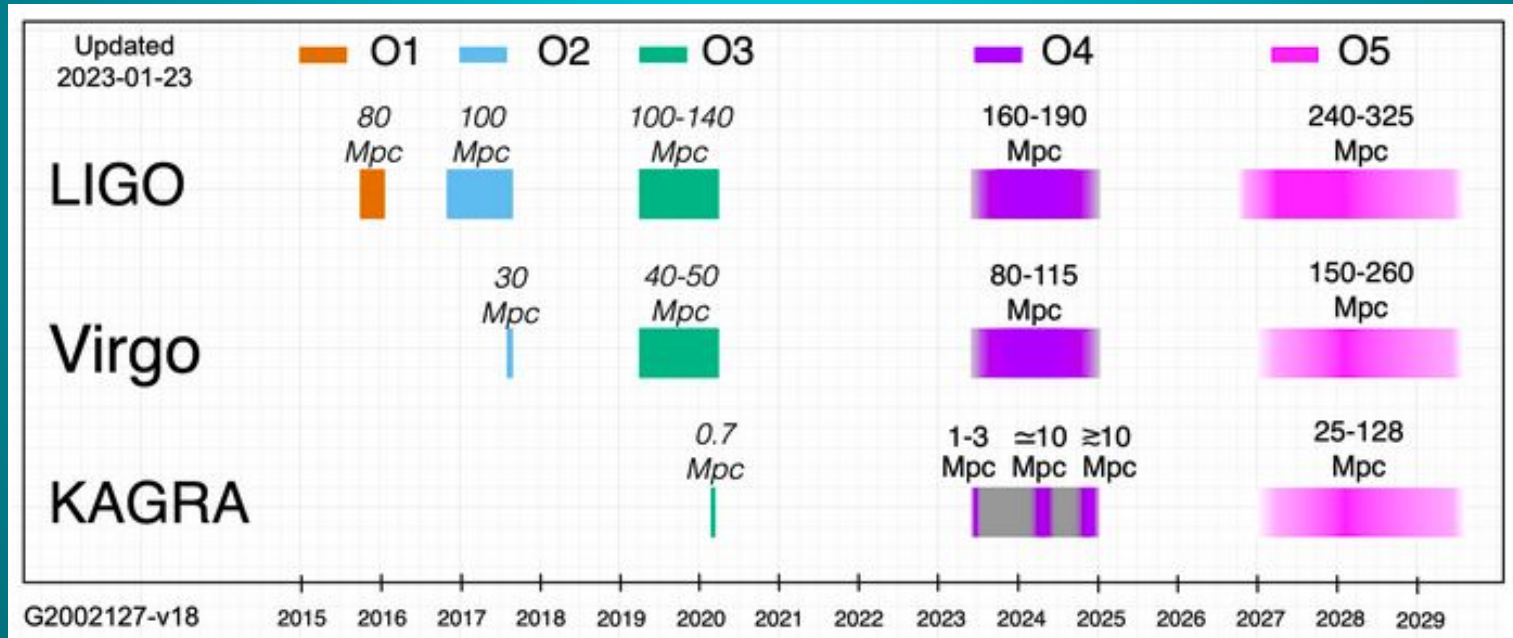
- Frequency dependent noise floor, we lose sensitivity in the kHz region.
- Vertical spikes in the spectrum are usually known noise sources (violin modes, calibration lines, etc.)
- We standardize the sensitivity by the distance at which a binary neutron star merger (1.4 solar masses) can be detected with SNR = 8.



# Run Sensitivities

1 parsec = 3.26 light-years

Milky Way Galaxy is ~30 kpc in diameter





# LSC Fellow work at Hanford

- 3 quarters; summers of 2018 and 2019, and winter of 2018.
- Helped with upgrades of physical environmental monitoring channels, and injection studies
- Commissioning projects aimed at maximizing the sensitivity in O3.

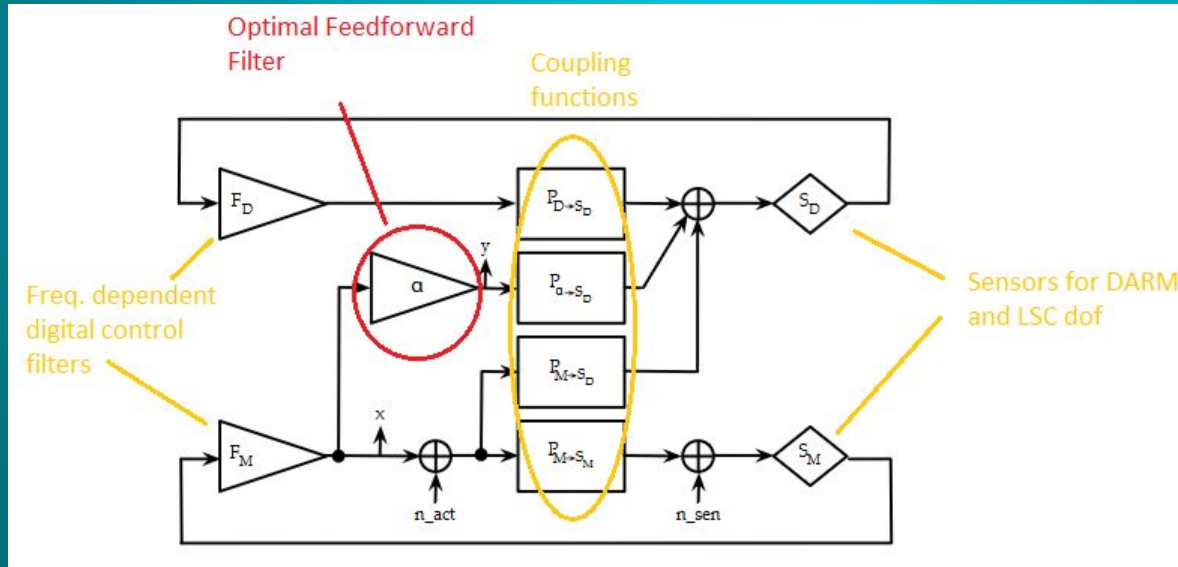


# Feedforward Filters

There are 3 Length Sensing and Control (LSC) degrees of freedom, any of which could couple to DARM and add noise.

1. Power Recycling Cavity Length (PRCL)
2. Signal Recycling Cavity Length (SRCL)
3. Michelson length (MICH)

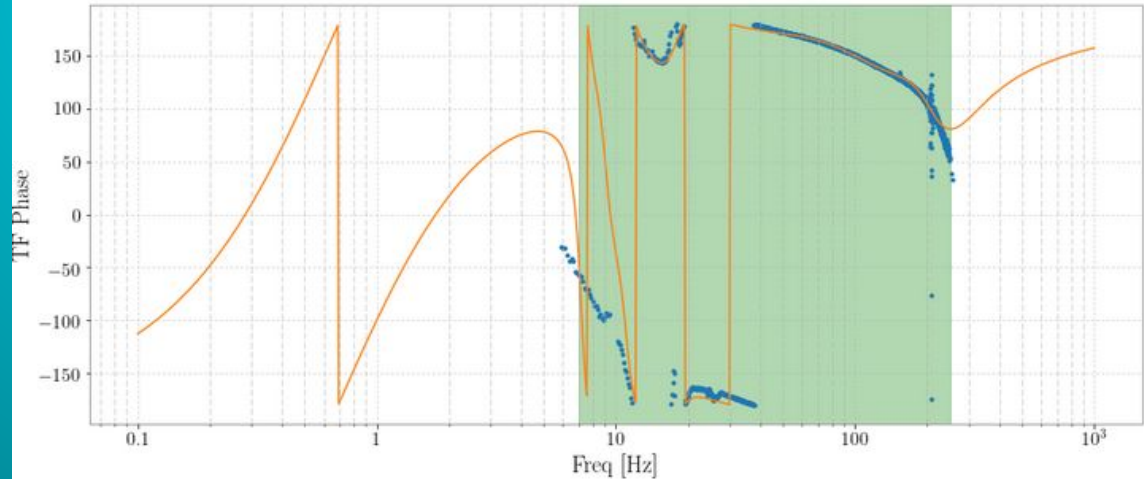
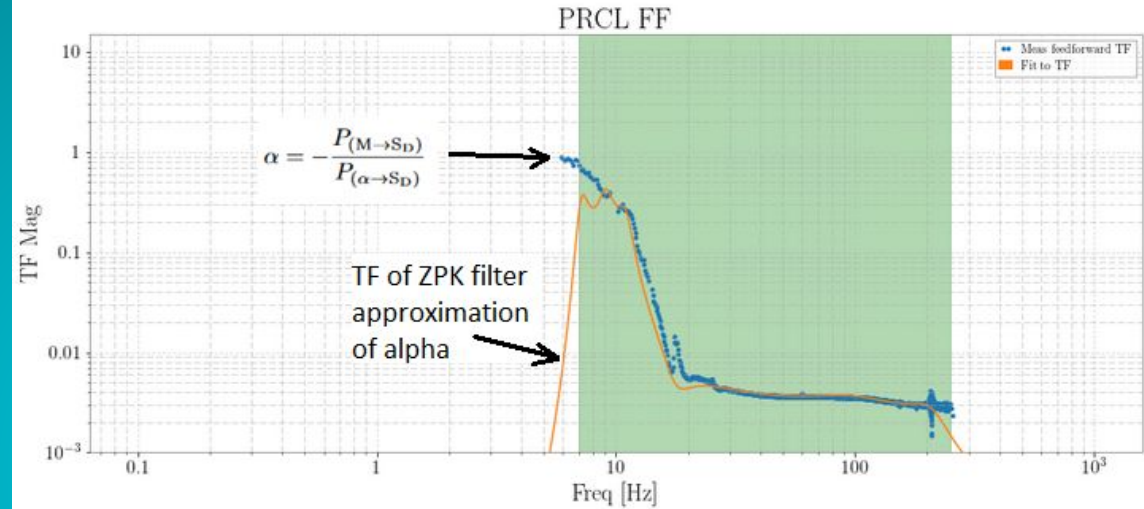
Goal: to design a filter,  $\alpha$ , that allows us to actuate differentially on the ITMs and cancel out the effects of  $n_{\text{sen}}$  (noise of LSC dof's)



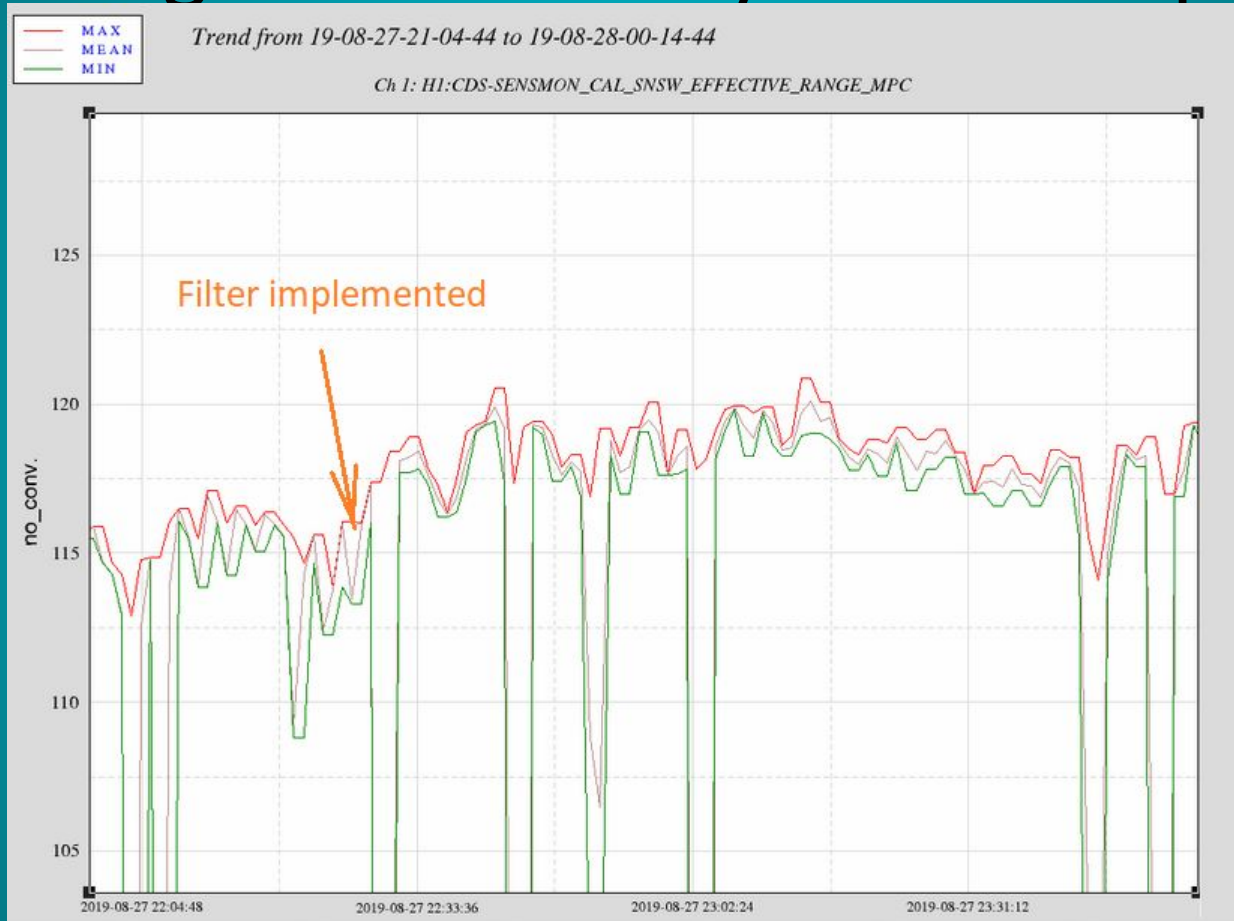
$$\alpha = -\frac{P_{(M \rightarrow S_D)}}{P_{(\alpha \rightarrow S_D)}}$$

# Transfer Function of Optimal Filter

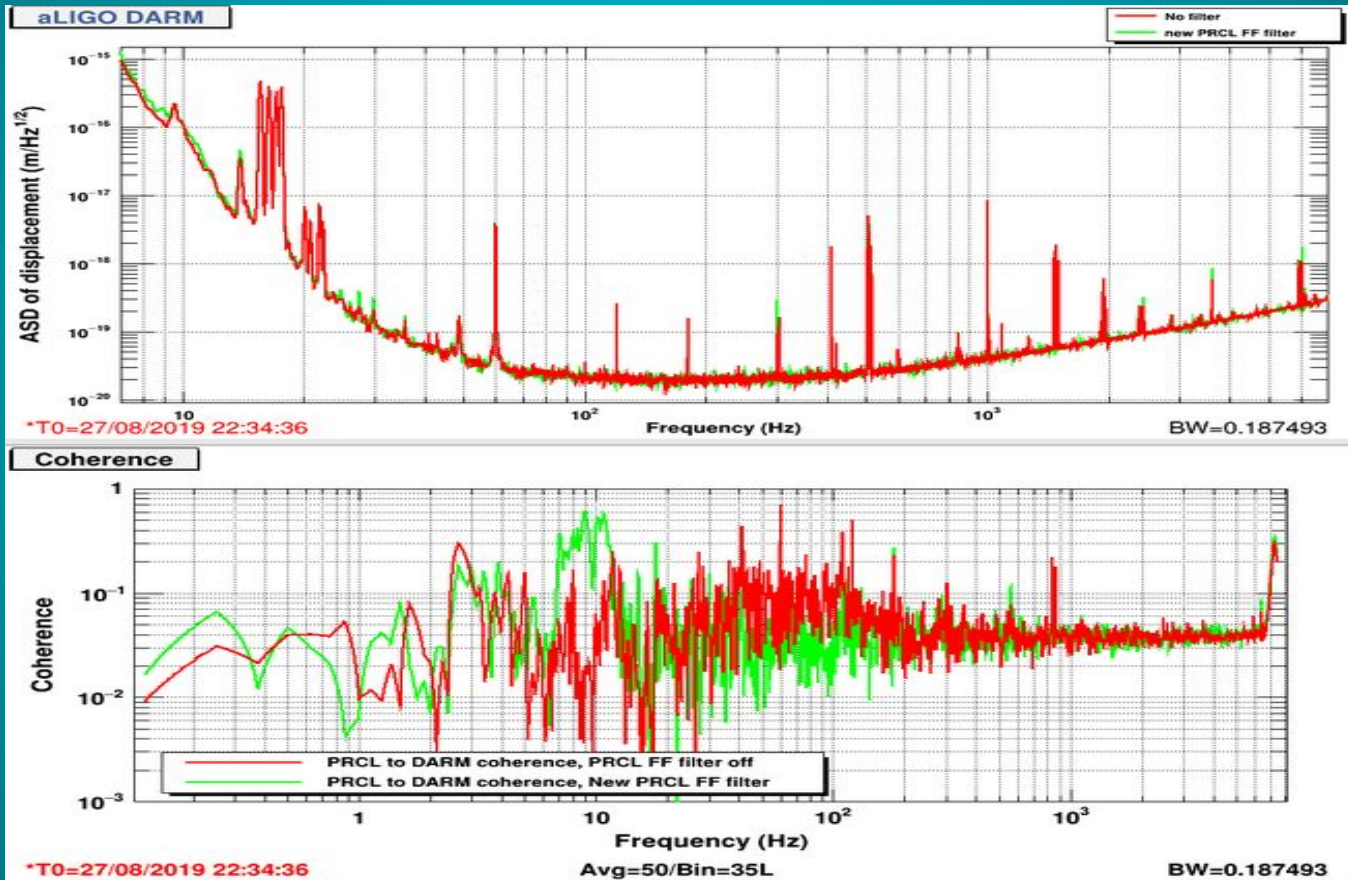
- The optimal alpha (blue) is measured through injections
- We only care about the filter in the shaded green region, where the highest coupling is, outside of that we only care that the magnitude of the transfer function drops off to zero



# Range Increased by about 2Mpc



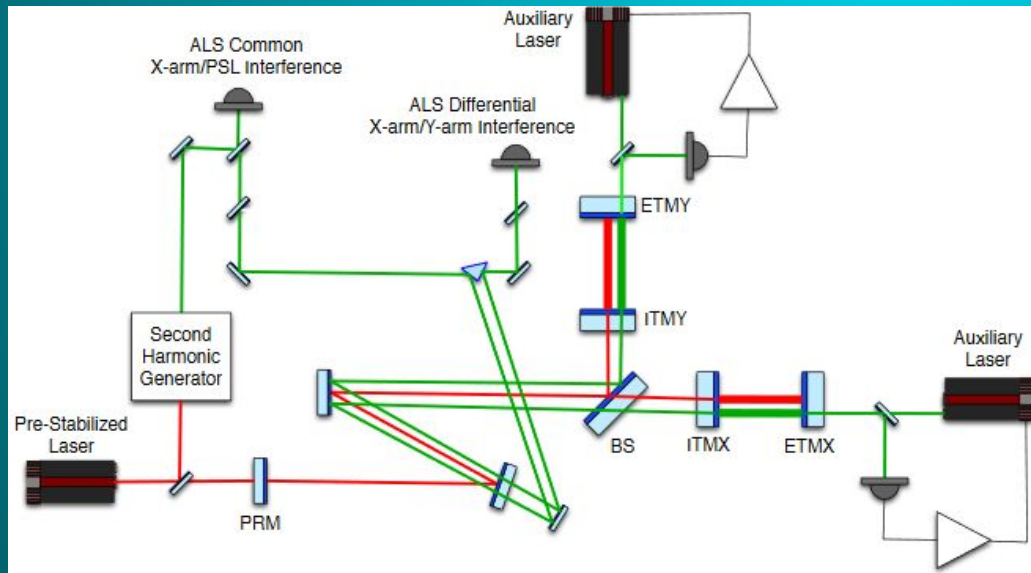
# A reduction in Coherence:



# Arm Length Stabilization (ALS) Locking

Locking: the process of controlling each cavity length such that they are all resonant.

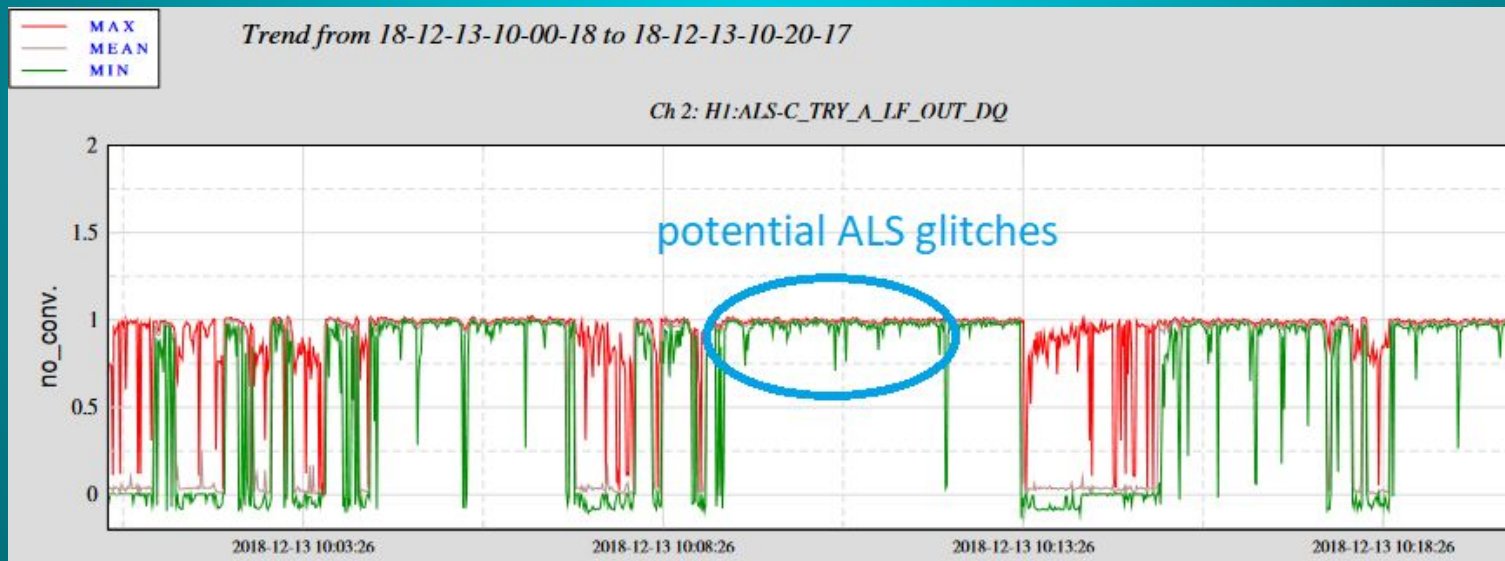
We maximize observation time by making the locking sequence more efficient.



- ALS lasers locked to the cavities at wavelength 532nm.
- Arm lengths measured in common and differential modes
- Common and differential mode control loops used to bring the common mode frequency offset between the ALS laser and the main laser to zero.

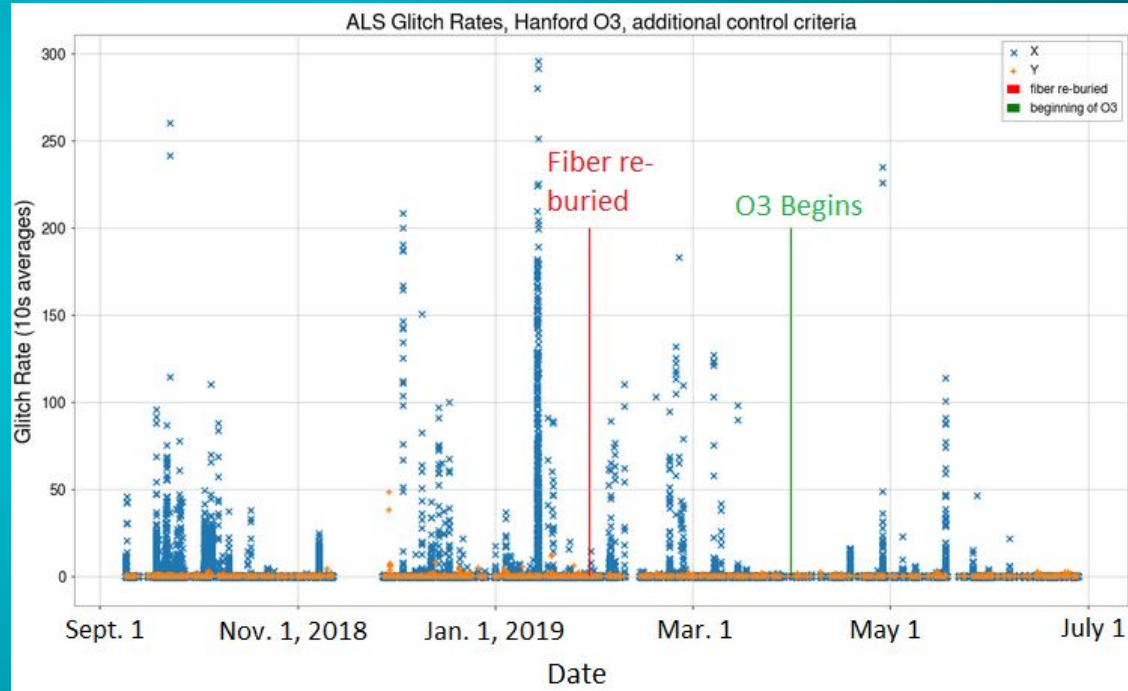
# Complications in ALS feedback loops: Glitches

ALS locking was complicated by sudden, high-frequency drops in the transmission signal for both X and Y arms. The commissioners anecdotally described these being more of a problem on rainy days.



# Identifying and mitigating the glitches:

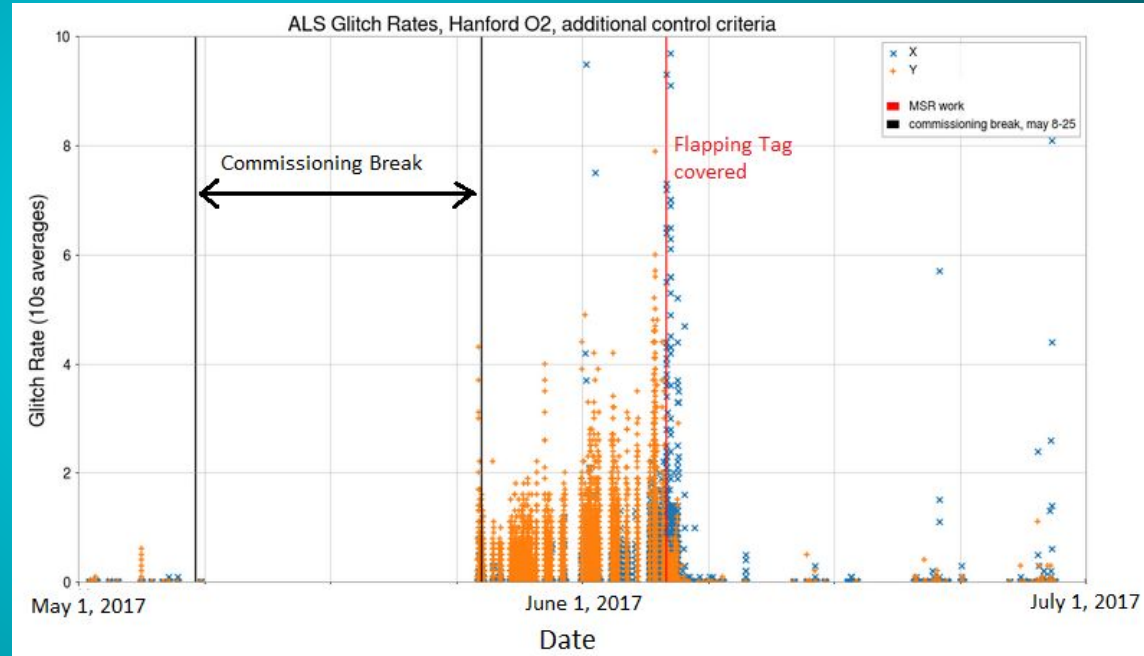
- I wrote code to identify the glitches, and searched for correlation with PEM channels, found none.
- Found no improvement in the glitch rates when the ALS fiber was re-buried, saved the lab ~\$100k on a new fiber.
- Re-ran the analysis on O2, identified a start date of the glitches, and improvement when a specific flapping tag was covered. These are likely the effect of a mechanical disturbance.





# Identifying and mitigating the glitches:

- I wrote code to identify the glitches, and searched for correlation with PEM channels, found none.
- Found no improvement in the glitch rates when the ALS fiber was re-buried, saved the lab ~\$100k on a new fiber.
- Re-ran the analysis on O2, identified a start date of the glitches, and improvement when a specific flapping tag was covered. These are likely the effect of a mechanical disturbance.



# Magnetar Overview

- Neutron Stars with exceptionally strong external dipole magnetic fields,  $\sim 10^{14}$ - $10^{15}$  G. Potentially stronger internal toroidal magnetic fields.
- Exhibit intermittent x-ray flaring activity, with energies up to  $\sim 10^{42}$  erg. Very rare 'giant flares' of energy up to  $\sim 10^{46}$  erg. Some are known to emit in radio frequencies as well.
- The flaring mechanism in a magnetar is not well understood, but theories include crust cracking, magnetic reconnection, hydrodynamic deformation, etc.
- If the flare excites non-radial modes (especially f-modes), then GWs might be produced. F-modes are the fundamental pressure mode,  $\sim 1$ -3 kHz.
- Magnetars are one of the leading progenitor models of Fast Radio Bursts (FRBs, ms duration, high-energy radio bursts from well outside our galaxy)
- $\sim 30$  known galactic magnetars.

Halloween 2022:



# Halloween 2022:

Not pictured: a Fast Radio Burst gun.

A lot of people in Co. Mayo, Ireland, learned a little bit about something they'll never need to know.

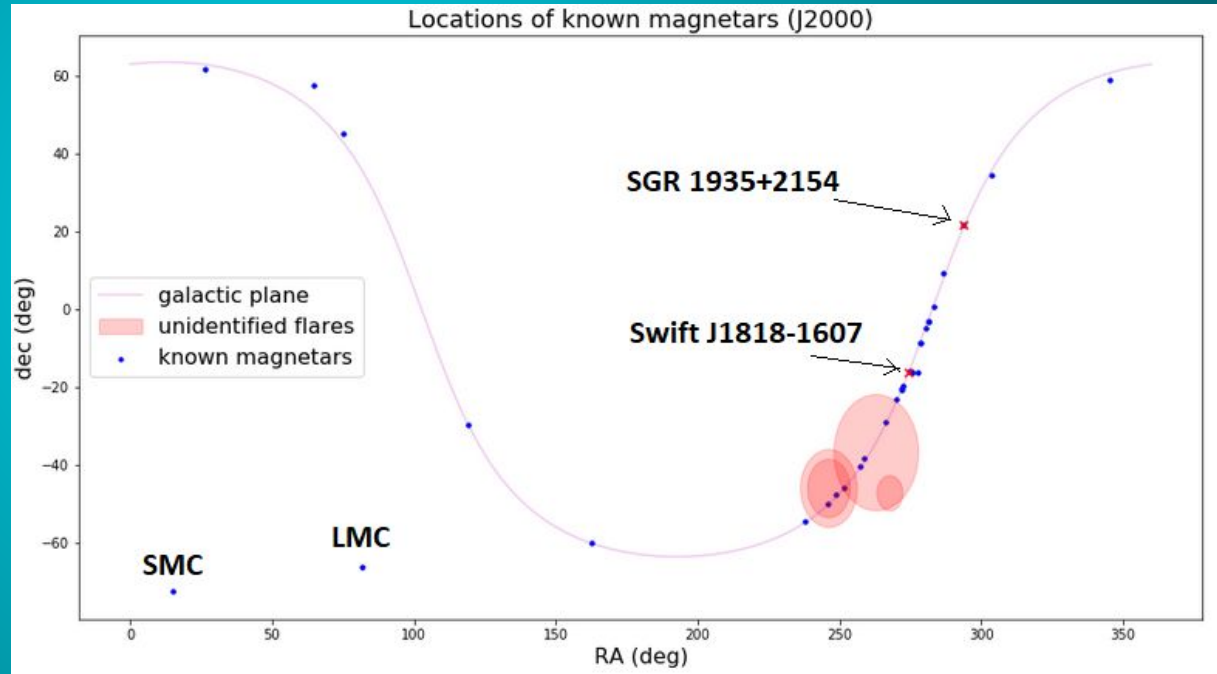


Co-artist:  
Ruby Stunton

# Magnetar Flares during O3

**16** flares total with multiple detectors in observing mode at the time of the flare.

- **2** flares from newly discovered magnetar Swift J1818-1607
- **11** flares from SGR 1935+2154
- **3** flares detected by Fermi from an unknown source

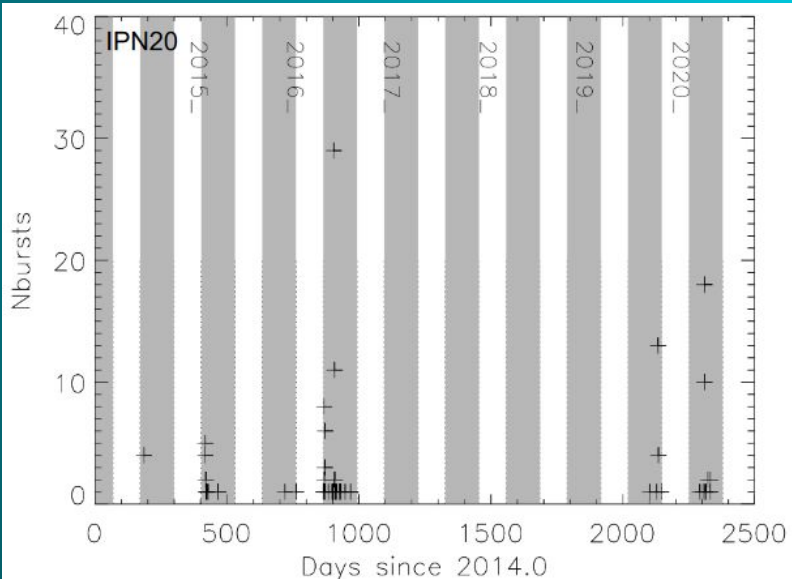


# Magnetar Flares during O3

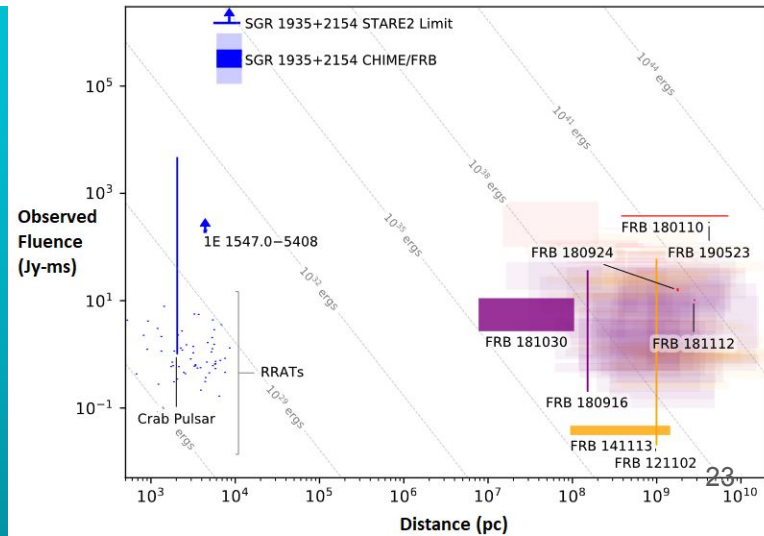
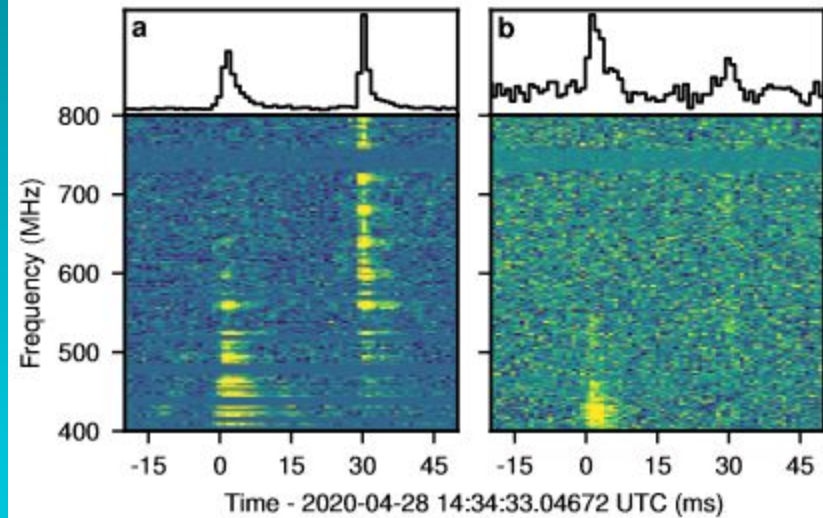
Burst	Source	Date	Time (UTC)	Detectors	$E_{EM}^{iso}$ (erg)	GCN Circulars
2651	SGR 1935+2154	Nov 04, 2019	01:54:37	H V*	-	26169
2652	SGR 1935+2154	Nov 04, 2019	02:53:31	H V	$1.4 \times 10^{39}$	26163, 26151
2653	SGR 1935+2154	Nov 04, 2019	04:26:55	H L V	$1.1 \times 10^{39}$	26163
2654	SGR 1935+2154	Nov 04, 2019	06:34:00	H L V	-	26153
2655	SGR 1935+2154	Nov 04, 2019	09:17:53	H L	$5.7 \times 10^{39}$	26163, 26154
2656	SGR 1935+2154	Nov 04, 2019	10:44:26	H L	$2.2 \times 10^{40}$	26242, 26163, 26158, 26157
2657	SGR 1935+2154	Nov 04, 2019	12:38:38	H L V	$2.7 \times 10^{39}$	26163
2660	SGR 1935+2154	Nov 04, 2019	15:36:47	H V	$1.2 \times 10^{39}$	-
2661	SGR 1935+2154	Nov 04, 2019	20:29:39	H V	$1.3 \times 10^{39}$	26165, 26166
2665	SGR 1935+2154	Nov 05, 2019	06:11:08	H V	$7.8 \times 10^{40}$	26242
2668	SGR 1935+2154	Nov 15, 2019	20:48:41	L V	$7.7 \times 10^{38}$	-
2669	-	Feb 03, 2020	03:17:11	H L V	-	26980
2670	-	Feb 03, 2020	03:44:03	H L V	-	26969, 26980
2671	-	Feb 03, 2020	20:39:37	H L V	-	26980
2673	Swift J1818.0-1607	Feb 28, 2020	22:19:32	L V	-	-
2674	Swift J1818.0-1607	Mar 12, 2020	21:16:47	H L V	-	27373

# SGR 1935+2154 emitted a galactic FRB, and has displayed possible periodic windowed behavior (PWB)

Grossan, B. 2021, Publications of the Astronomical Society of the Pacific, 133, 074202



CHIME/FRB  
Collaboration et al. 2020,  
Nature, 587, 54:



# Search Structure - 2 part search

- Targeted searches - we know exact points in the sky so we can gain sensitivity by coherently combining the data streams
- We know the time of the flares, so we can define a time-period around that (the on-source) where we search for a GW.

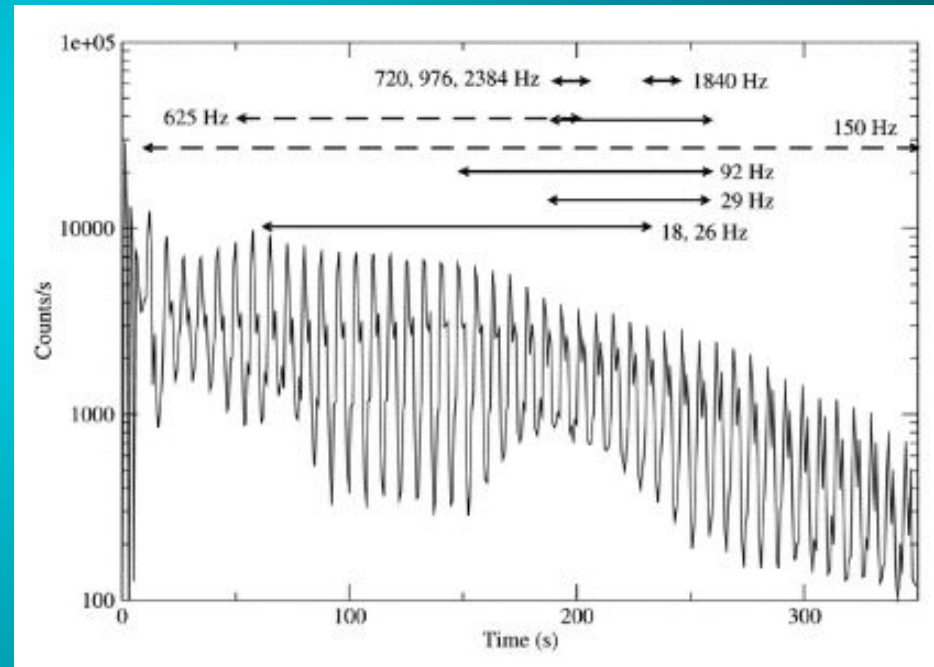
$$p = \frac{N_{\geq}}{N_{\text{total}}}$$

## Long- duration search:

- Search for signals ~100s of seconds long and changing minimally in frequency
- Search in [+4s, 1604s] after the flare
- Motivated by the quasiperiodic oscillations observed in the tails of giant flares

## Short-duration search:

- Search for signals (ms to s), any frequency morphology
- We search in [-4s, +4s] and [+4s,+504s] around the flare time.
- Trying to detect excited f-modes both at the flare time, and during the QPOs.





# Search Sensitivity estimation

We standardize the sensitivity of the search by injecting waveforms into the data, and noting the root sum squared injection amplitude ( $h_{\text{rss}}$ ) at which 50% are recovered ( $h_{\text{rss}}^{50\%}$ ).

We can approximate a corresponding gravitational-wave energy if we assume a distance to the source.

For both the short and long-duration searches, waveforms include sine-Gaussians and ringdowns. The short-duration search also includes white noise bursts.

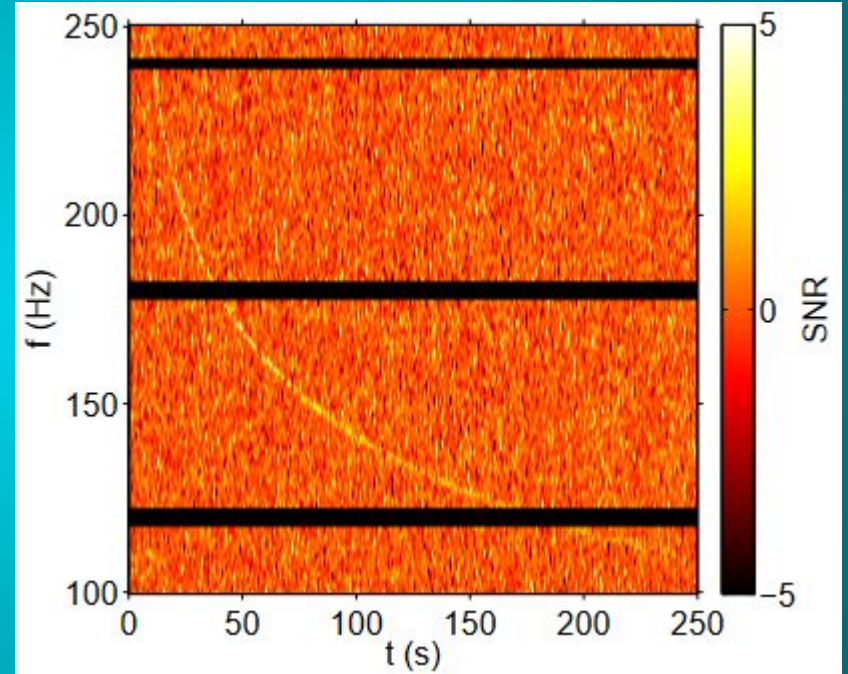
$$h_{\text{rss}} = \sqrt{\int_{-\infty}^{\infty} |h_+(t)|^2 + |h_\times(t)|^2 dt}$$

$$E_{\text{GW}} \approx \frac{2}{5} \frac{c^3 \pi^2}{G} d^2 f_0^2 h_{\text{rss}}^2$$

# Long-Duration search

## Methods:

- We used the Stochastic Transient Analysis Multi-detector Pipeline (STAMP)
- Data is broken into an on-source and background time-frequency maps, each pixel has an SNR
- 2nd order Bezier curves are generated over these TF maps, each is assigned an SNR based on the pixels it crosses.
- The loudests cluster in the on-source is then compared to the loudest cluster in each background segment
- Search in [+4s, +1604s] after the flare
- 24 Hz - 2500 Hz
- We inject waveforms to determine the  $h_{\text{rss}}$  at which we recover an injection with 50% efficiency ( $h_{\text{rss}}^{50\%}$ ).



# Long-Duration search results

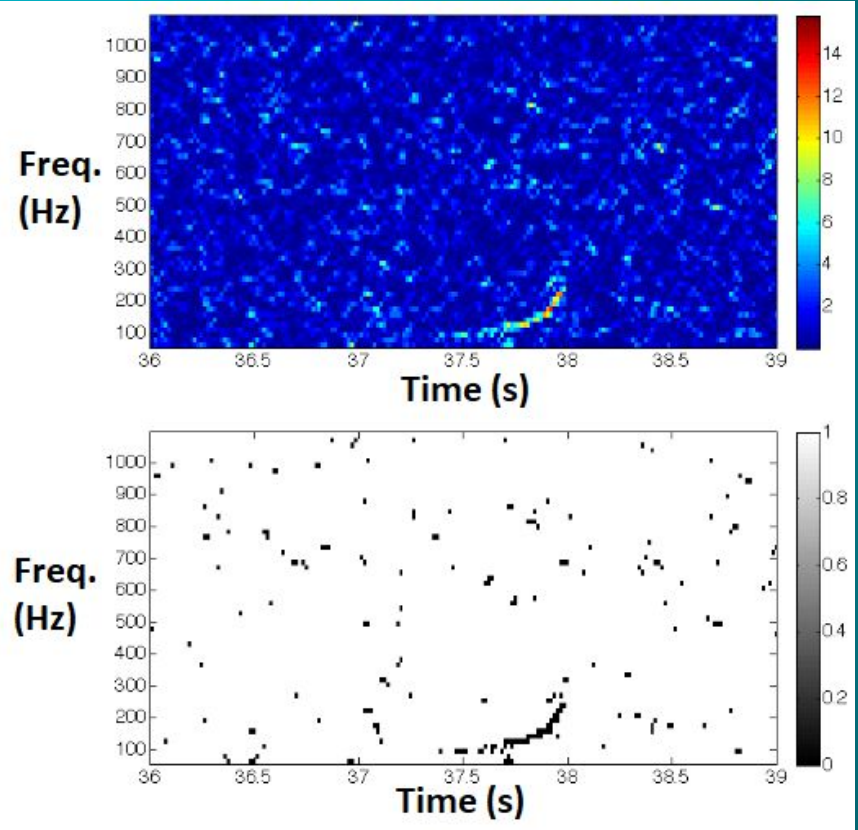
- No low p-value events
- We compute the  $h_{\text{rss}}^{50\%}$  for Ringdown and Half Sine-Gaussian waveforms, and the corresponding energy.
- We present the most sensitive results from SGR 1818.0-1607 (assuming distance = 4.8 kPc).

Frequency (Hz)	$\tau$ (s)	Half Sine-Gaussian			Ringdown		
		Burst	$h_{\text{rss}}^{50\%}$ ( $\text{Hz}^{-1/2}$ )	$E_{\text{GW}}^{50\%}$ (erg)	Burst	$h_{\text{rss}}^{50\%}$ ( $\text{Hz}^{-1/2}$ )	$E_{\text{GW}}^{50\%}$ (erg)
55	150	2674	$1.6 \times 10^{-22}$	$2.8 \times 10^{43}$	2674	$1.7 \times 10^{-22}$	$3.1 \times 10^{43}$
	400	2673	$1.9 \times 10^{-22}$	$3.7 \times 10^{43}$	2673	$2.0 \times 10^{-22}$	$4.1 \times 10^{43}$
150	150	2674	$1.3 \times 10^{-22}$	$1.3 \times 10^{44}$	2674	$1.4 \times 10^{-22}$	$1.5 \times 10^{44}$
	400	2674	$1.4 \times 10^{-22}$	$1.5 \times 10^{44}$	2674	$1.4 \times 10^{-22}$	$1.6 \times 10^{44}$
450	150	2674	$1.2 \times 10^{-22}$	$1.1 \times 10^{45}$	2674	$1.3 \times 10^{-22}$	$1.2 \times 10^{45}$
	400	2674	$1.5 \times 10^{-22}$	$1.6 \times 10^{45}$	2674	$1.6 \times 10^{-22}$	$1.8 \times 10^{45}$
750	150	2674	$2.0 \times 10^{-22}$	$8.1 \times 10^{45}$	2674	$2.2 \times 10^{-22}$	$9.6 \times 10^{45}$
	400	2674	$2.2 \times 10^{-22}$	$9.9 \times 10^{45}$	2674	$2.4 \times 10^{-22}$	$1.1 \times 10^{46}$
1550	150	2674	$5.7 \times 10^{-22}$	$2.7 \times 10^{47}$	2674	$5.6 \times 10^{-22}$	$2.6 \times 10^{47}$
	400	2674	$4.9 \times 10^{-22}$	$2.0 \times 10^{47}$	2674	$5.0 \times 10^{-22}$	$2.1 \times 10^{47}$

# O3 Short-duration search Methods

**X-pipeline:** coherent search pipeline, used for short-duration (ms to s) signals, loses sensitivity to longer signals.

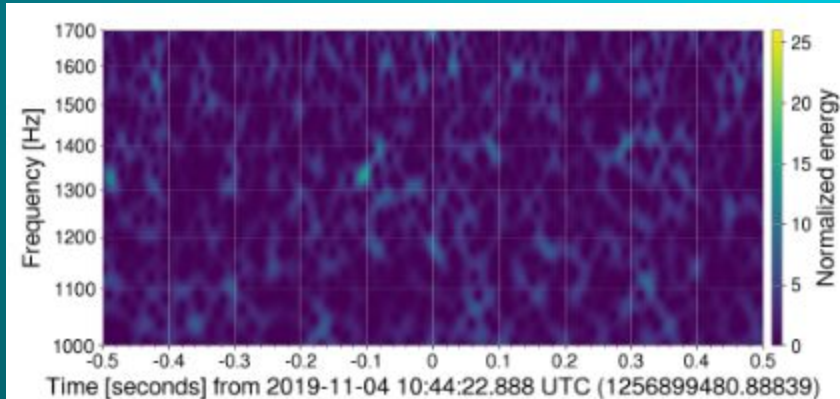
- Combines data from all detectors into a time-frequency map, where each pixel has an associated significance
- Selects out the brightest 1% of pixels, and groups neighboring pixels into clusters. Each cluster's significance is the sum of its constituent pixels.
- Each cluster in the on-source is treated as a potential gravitational-wave, and its properties compared to those in the background
- 50 Hz - 4000 Hz



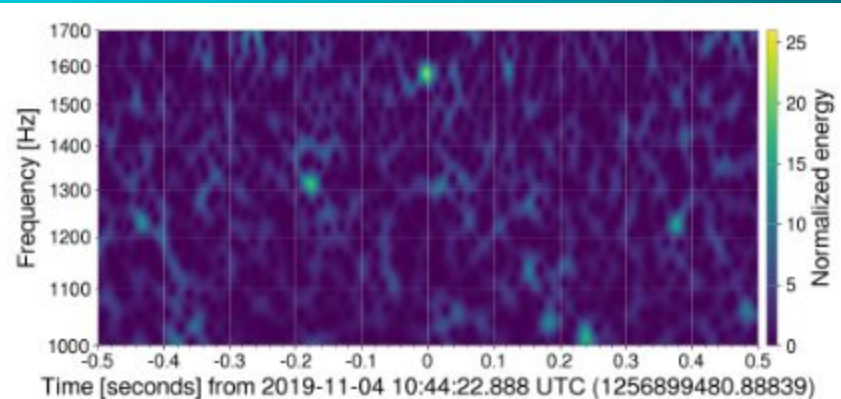
# Short-Duration Search Results

- Lowest p-value =  $8.6 \times 10^{-3}$ ,  $f = 1560\text{--}1608$  Hz, duration = 63 ms, Burst 2656 from SGR 1935+2154
- Sensitivity of Burst 2656:  $h_{\text{rss}}^{50\%} = 2.1 \times 10^{-22} \text{ Hz}^{-1/2}$ ,  $E_{\text{GW}}^{50\%} = 1.4 \times 10^{47} \text{ erg}$
- GW/EM energy ratio =  $10^6$ . Injected waveforms are Ringdowns at  $f = 1590$  Hz, duration = 100 ms.

LIGO Hanford



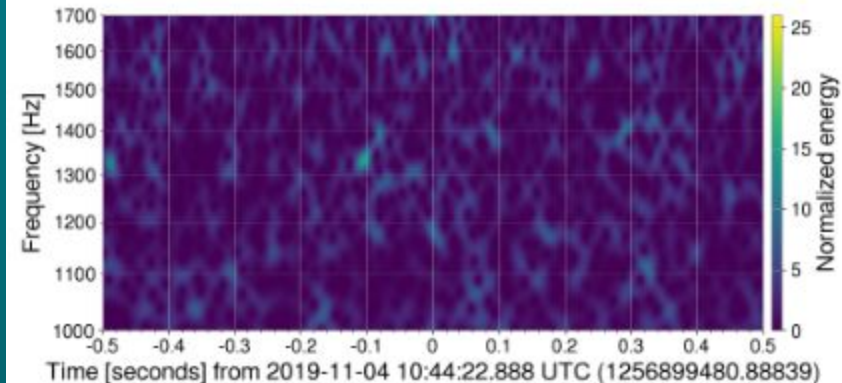
LIGO Livingston



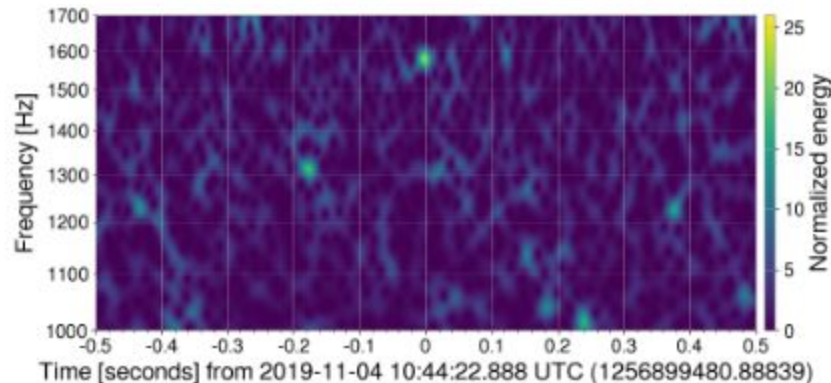
# Short-Duration Search Results

- The loud event happened  $\sim 3.1$  s before the x-ray burst. Inconsistent with astrophysical models.
- Given the number of analyses we ran, probability of this low p-value is  $\sim 29\%$ .
- Much louder in Livingston, most likely an instrumental artifact.

LIGO Hanford



LIGO Livingston



# Short-Duration Search Sensitivity

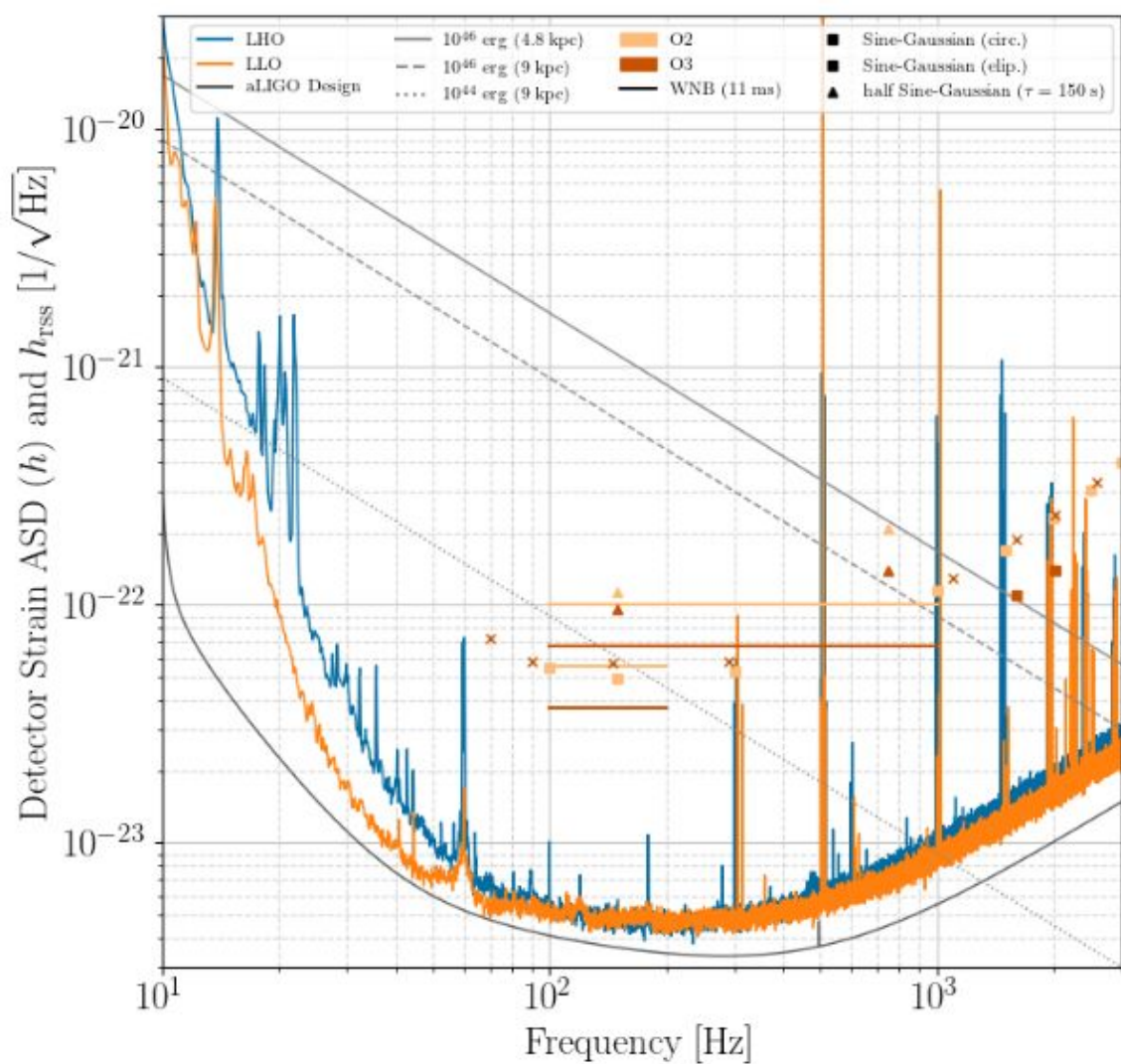
Ringdowns at  
1590 Hz, 100 ms

Sine Gaussians  
at 1600 Hz, 6.25  
ms.

Burst	Source	Ringdowns		Sine Gaussians	
		$E_{\text{GW}}^{50\%}$ (erg)	Eratio	$E_{\text{GW}}^{50\%}$ (erg)	Eratio
2652	SGR 1935+2154	$3.2 \times 10^{47}$	$2.2 \times 10^8$	$8.0 \times 10^{46}$	$5.6 \times 10^7$
2653	SGR 1935+2154	$2.2 \times 10^{47}$	$1.9 \times 10^8$	$7.3 \times 10^{46}$	$6.4 \times 10^7$
2654	SGR 1935+2154	$7.8 \times 10^{47}$	-	$2.7 \times 10^{47}$	-
2655	SGR 1935+2154	$1.1 \times 10^{47}$	$1.9 \times 10^7$	$3.8 \times 10^{46}$	$6.6 \times 10^6$
2656	SGR 1935+2154	$1.4 \times 10^{47}$	$6.4 \times 10^6$	$4.9 \times 10^{46}$	$2.2 \times 10^6$
2657	SGR 1935+2154	$1.8 \times 10^{47}$	$6.6 \times 10^7$	$6.4 \times 10^{46}$	$2.3 \times 10^7$
2660	SGR 1935+2154	$3.6 \times 10^{47}$	$3.0 \times 10^8$	$1.3 \times 10^{47}$	$1.1 \times 10^8$
2661	SGR 1935+2154	$3.2 \times 10^{47}$	$2.4 \times 10^8$	$1.2 \times 10^{47}$	$9.0 \times 10^7$
2668	SGR 1935+2154	$1.4 \times 10^{47}$	$1.8 \times 10^8$	$4.6 \times 10^{46}$	$6.0 \times 10^7$
2669	unknown	$7.3 \times 10^{45}$	-	$2.2 \times 10^{45}$	-
2670	unknown	$6.8 \times 10^{45}$	-	$2.5 \times 10^{45}$	-
2671	unknown	$2.2 \times 10^{46}$	-	$7.9 \times 10^{45}$	-
2673	Swift J1818-1607	$6.6 \times 10^{46}$	-	$2.0 \times 10^{46}$	-
2674	Swift J1818-1607	$3.8 \times 10^{46}$	-	$1.2 \times 10^{46}$	-

## Comparing to O2 Sensitivity:

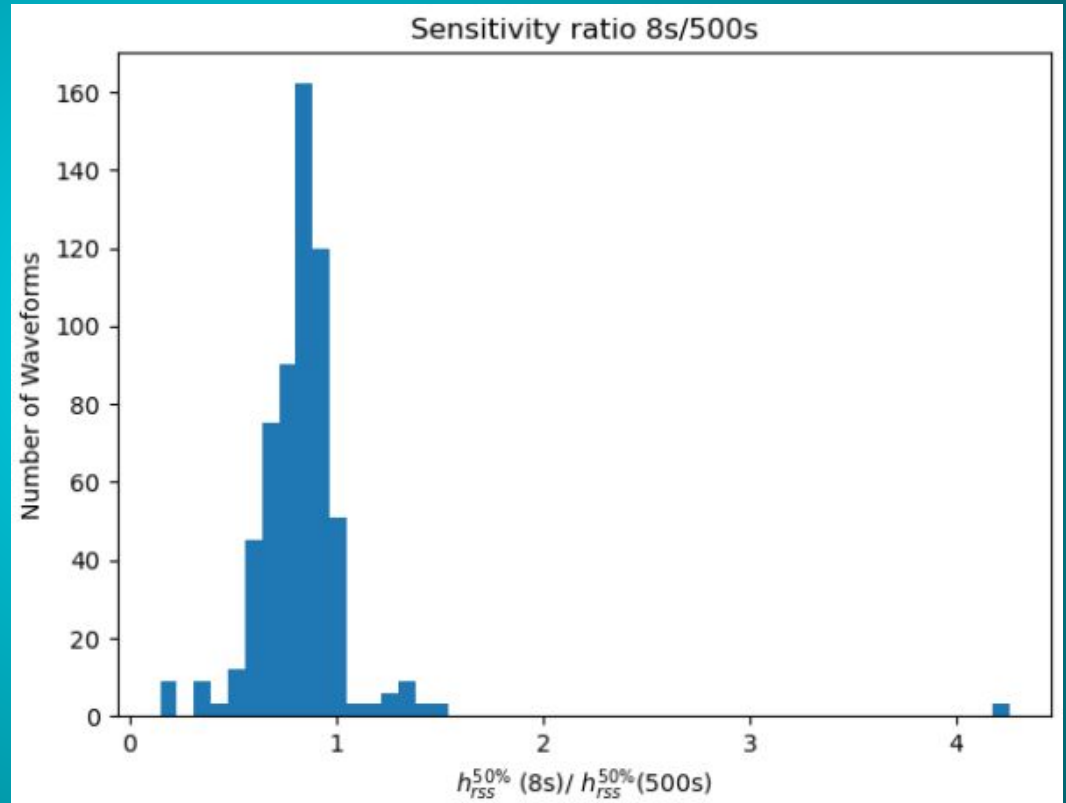
- We moved the injections off of the violin mode frequencies
- For the short-duration search, injections were elliptically polarized in O3, circularly polarized in O2. Circularly polarized SG's at 1600 Hz and 2020 Hz, factors of improvement of 1.5 and 1.7 respectively





# Effectiveness of two separate on-source windows

The median  $h_{rSS}^{50\%}$  for the 8s search is 83% that of the 500s search



## O3a Fast Radio Burst (FRB) search

- Short (ms duration) bright radio bursts with dispersion measures indicating sources well outside our galaxy
- 2 classes: repeaters and non-repeaters
- Interesting properties - one FRB has a periodicity of  $\sim 16$  days, and another has periodic windowed behavior with period=157 days.
- FRB progenitors are not well known, but magnetars are a leading candidate for repeaters

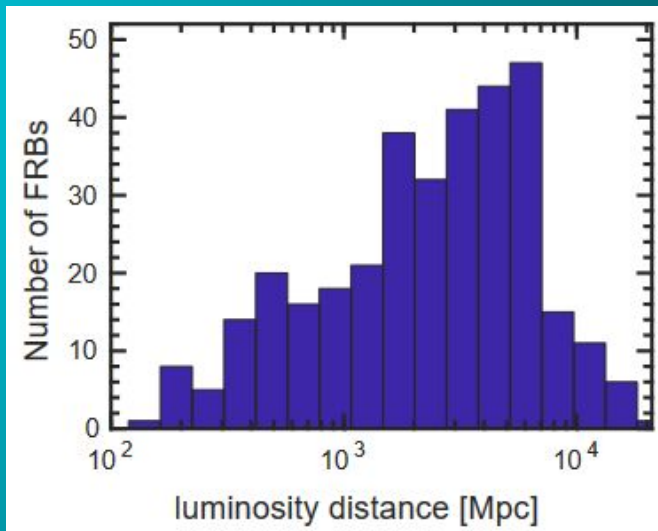
# Canadian Hydrogen Intensity Mapping Experiment (CHIME)

- Radio telescope, began commissioning in 2018.
- 200 sq. deg. field of view
- Lower frequency range, 400-800 MHz.
- Has made thousands of FRB detections since 2018.



<https://chime-experiment.ca/>

Chime released information on 806 FRBs (338 from O3a) to the LVK for the O3 search.



# Search over repeating FRBs: x-pipeline

- X-pipeline analysis was reminiscent of that of the O3 magnetar search
- The distance estimates are too high to place meaningful upper limits on the gravitational-wave energy.

FRB Name	UTC Time [s]	R.A.	Dec.	Network	DM [pc cm <sup>-3</sup> ]	$D_L$ -Low [Mpc]	$D_L$ -high [Mpc]
FRB20190817A	14:39:52	4 <sup>h</sup> 21 <sup>m</sup> 08 <sup>s</sup>	73°47'	H1L1V1	189.5	19.5	539.2
FRB20190929C	11:58:29	4 <sup>h</sup> 22 <sup>m</sup> 25 <sup>s</sup>	73°40'	H1L1V1	191.6	20.8	550.1
FRB20190518A	18:13:33	1 <sup>h</sup> 58 <sup>m</sup> 14 <sup>s</sup>	65°46'	L1V1	350.5	148.1	149.9
FRB20190518E	18:20:57	1 <sup>h</sup> 57 <sup>m</sup> 50 <sup>s</sup>	65°43'	L1V1	350.0	148.1	149.9
FRB20190519A	17:50:16	1 <sup>h</sup> 43 <sup>m</sup> 44 <sup>s</sup>	65°48'	H1V1	350.0	148.1	149.9
FRB20190519C	18:10:41	1 <sup>h</sup> 58 <sup>m</sup> 00 <sup>s</sup>	65°47'	H1V1	348.8	148.1	149.9
FRB20190809A	12:50:40	1 <sup>h</sup> 58 <sup>m</sup> 16 <sup>s</sup>	65°43'	H1L1	356.2	148.1	149.9
FRB20190825A	11:48:18	1 <sup>h</sup> 58 <sup>m</sup> 07 <sup>s</sup>	65°42'	H1L1	349.6	148.1	149.9
FRB20190825B	11:51:54	1 <sup>h</sup> 58 <sup>m</sup> 04 <sup>s</sup>	65°23'	H1L1	349.9	148.1	149.9
FRB20190421A	08:00:04	13 <sup>h</sup> 51 <sup>m</sup> 57 <sup>s</sup>	48°10'	H1L1V1	225.9	125.1	1260.8
FRB20190702B	03:14:36	13 <sup>h</sup> 52 <sup>m</sup> 25 <sup>s</sup>	48°15'	L1V1	224.4	125.8	1257.5

# What to Expect in O4/O5:

- More flares from SGR 1935+2154. (All of the flares in O3 clustered around 4 Nov. 2019).
- Possibly another FRB from SGR 1935+2154 (although there is evidence for FRB/magnetar flare associations to be quite rare).
- We could gain sensitivity through ‘stacking’ the triggers (from the same source), and effectively raising the SNR of the stacked GW. Tentatively in plans for O4.

## X-PIPELINE STATUS & PLANS

P. SUTTON G2200255-V2

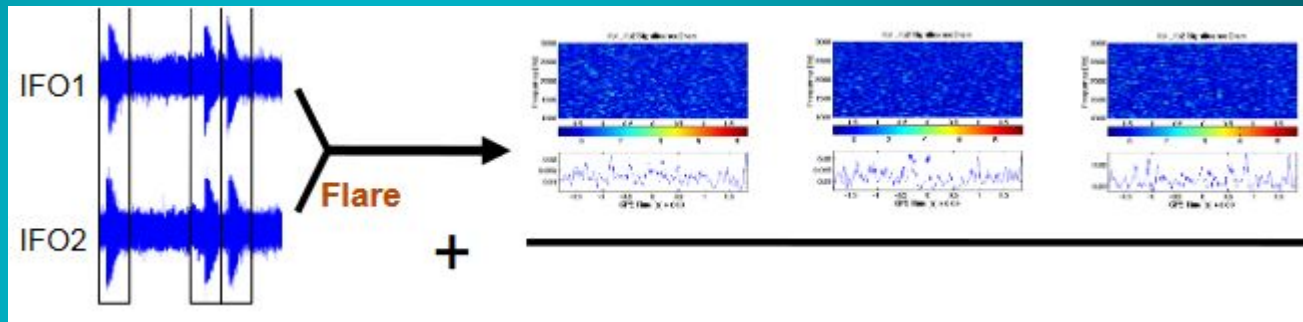
- Critical priorities:

1. Convert all python scripts from python2 to python3 [~one week]
2. Enable alerts to graced [not started]
3. Enable stacking for repeating FRBs and magnetars [not started – not needed for O4 start]

# Stacked Analysis: Previous studies by Peter Kalmus (S6) in 2009

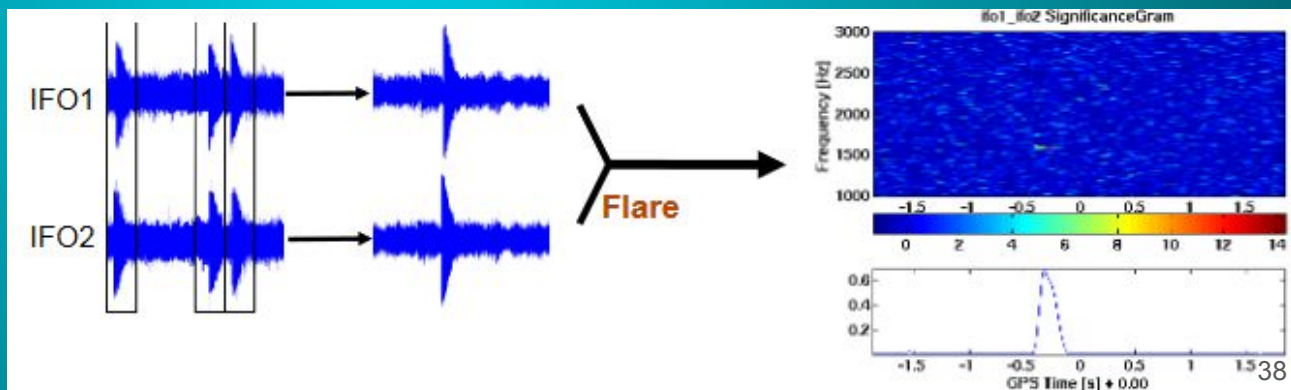
## Power-Stacking:

- Make 1 time-frequency map per trigger, and stack the TF maps
- Sensitivity  $\sim N^{1/4}$
- Allows for uncertainty in arrival times



## Time-Stacking:

- Combines timeseries data, makes one TF map
- Greater sensitivity  $\sim N^{1/2}$
- If flares are out of phase they could interfere



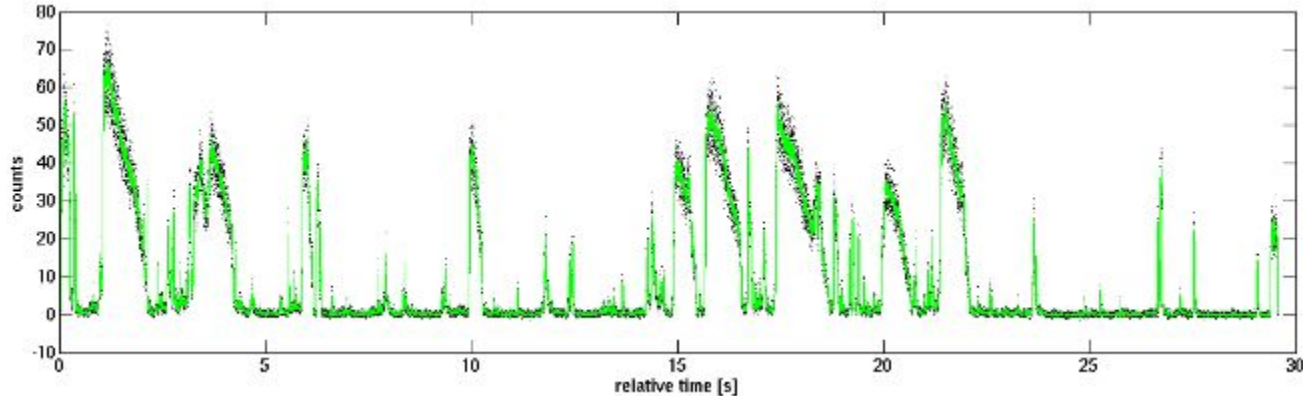
# Types of Flares to Stack:

Flare Storms: ~10s of flares in minutes

- SGR 1935+2154 at the time of FRB
- Kalmus's analysis handled an instance of this:

Spread Out Flares: ~10s of flares in a couple of days/weeks

- SGR 1935+2154 in O3
- Swift J1818.0-1607 in O3
- Most repeating FRBs



Each class may or may not have the same internal driving mechanism. Our stacking method should be able to handle both together, or either one separately.

# X-pipeline Modifications to handle Stacking:

Currently, X-pipeline runs as a 2-part search

- 1st stage: Identifies loud clusters and assigns each a series of properties (SNR, different measures of energy, peak time, peak frequency, etc.)
- 2nd stage: takes the list of loud clusters and calculates optimal cuts to make based on WFs, signal consistency, etc.
- Uses these same cuts on the onsource and then looks at the most significant surviving triggers.



# X-pipeline Modifications to handle Stacking:

Currently, X-pipeline runs as a 2-part search

- 1st stage: Identifies loud clusters and assigns each a series of properties (SNR, different measures of energy, peak time, peak frequency, etc.)
- **Extra Step here for Stacking:** The onsource window is the time around each trigger (say -1s,+4s). So combine all the properties of the clusters within these times. List of offsource triggers would be generated the same way for equally spaced times in time-slid data.
- 2nd stage: takes the list of **stacked** clusters and calculates optimal cuts to make based on WFs, signal consistency, etc.
- Uses these same cuts on the onsource and then looks at the most significant surviving triggers.

# Statistics of what we actually stack:

- We end up with Time-Frequency bins, each of which has as its significance (SNR) the sum of the significances of all clusters from all triggers which fell into that TF bin.
- Some TF bins have a significance of 0, which is fine.
- We calculate a p-value by looking at the number of TF bins louder than a specific bin

$$P = \frac{\text{Number of TF bins louder than event}}{\text{Total TF bins}}$$

## How Precise Can we get?




- The limiting factor for the p-value (per frequency) is the number of time-bins available.
- Standard x-pipeline run has background length 10800s, we are using 64s blockTime (which implies five 3s circular timeslides, and 138 different 32s lags)
- Effective background time is  $10800 \cdot 138 \cdot 5 = 7,452,000\text{s}$ .  $\Rightarrow$  1,490,400 time-bins in each are 5s long.
- **Minimum possible p-value is  $P=6.7 \times 10^{-7}$**

We've made a stacking branch of X-pipeline with the infrastructure to do the added steps before the post-processing:

<https://trac.ligo.caltech.edu/xpipeline/browser/xpipeline/branches/stacking>

source: [xpipeline](#) / [branches](#) / [stacking](#)

Visit:

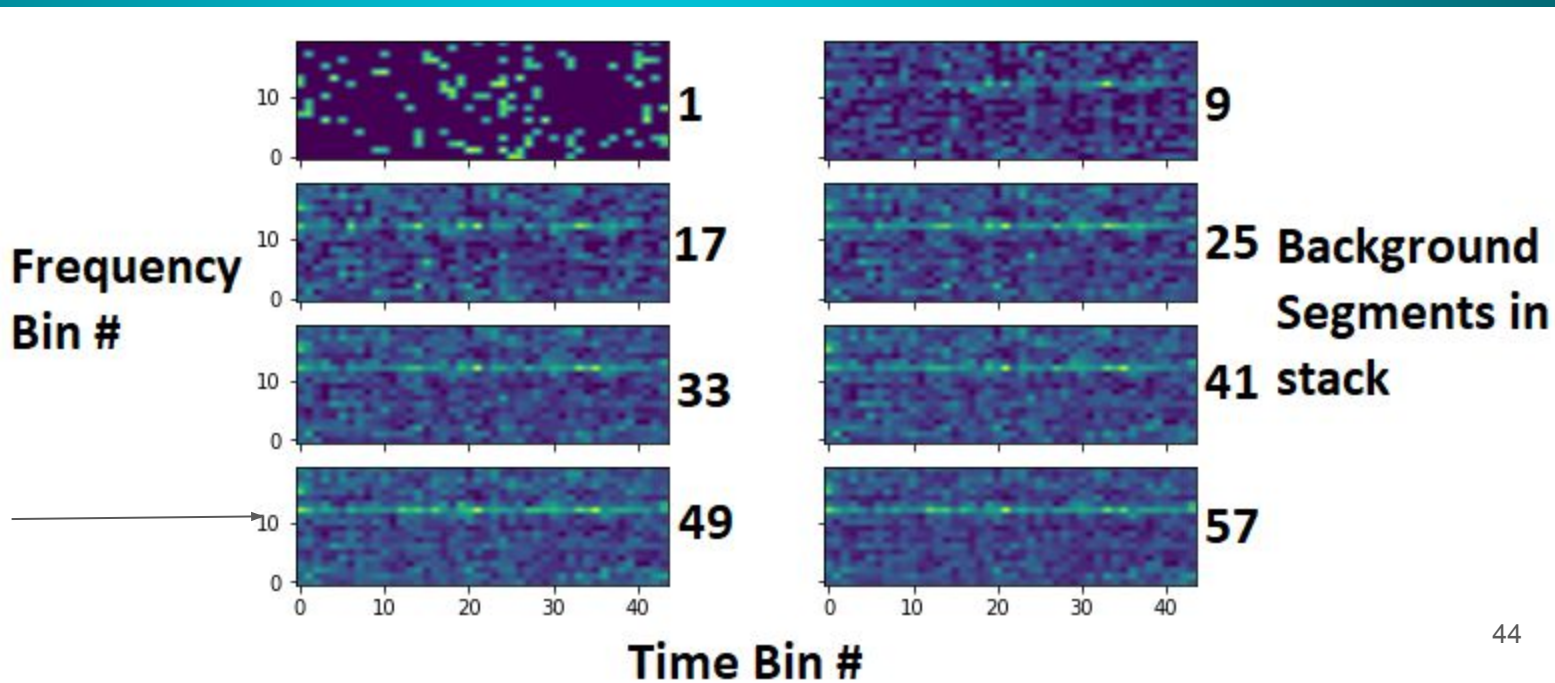
Name ▲	Size	Rev	Age	Author
 <a href="#">../</a>				
▶  <a href="#">auto_build</a>		<a href="#">6187</a> 	<a href="#">3 months</a>	<a href="#">patrick.sutton</a>
▶  <a href="#">dependencies</a>		<a href="#">6152</a> 	<a href="#">4 months</a>	<a href="#">patrick.sutton</a>
▶  <a href="#">m4</a>		<a href="#">6185</a> 	<a href="#">3 months</a>	<a href="#">patrick.sutton</a>
▶  <a href="#">matlab</a>		<a href="#">6259</a> 	<a href="#">3 weeks</a>	<a href="#">kara.merfeld</a>
 <a href="#">00boot</a>	145 bytes 	<a href="#">5421</a> 	<a href="#">6 years</a>	<a href="#">edward.daw</a>
 <a href="#">.gitignore</a>	122 bytes 	<a href="#">2070</a> 	<a href="#">15 years</a>	<a href="#">jrollins</a>
 <a href="#">clean_svnversion.sh</a>	611 bytes 	<a href="#">5695</a> 	<a href="#">3 years</a>	<a href="#">patrick.sutton</a>
 <a href="#">configure.ac</a>	2.4 KB 	<a href="#">5421</a> 	<a href="#">6 years</a>	<a href="#">edward.daw</a>
 <a href="#">Makefile.am</a>	173 bytes 	<a href="#">5421</a> 	<a href="#">6 years</a>	<a href="#">edward.daw</a>
 <a href="#">README</a>	1.9 KB 	<a href="#">6181</a> 	<a href="#">4 months</a>	<a href="#">patrick.sutton</a>

# A Very Preliminary Study:

- I took 57 background segments from the same trigger, pretended they were 57 different triggers, stacked them, and then plotted the energy in each Time-Frequency bin.
- 5s time-bins, 100Hz frequency bins (1kHz - 3kHz)
- X-pipeline does whiten the data, but some frequency bins still have disproportionately many clusters

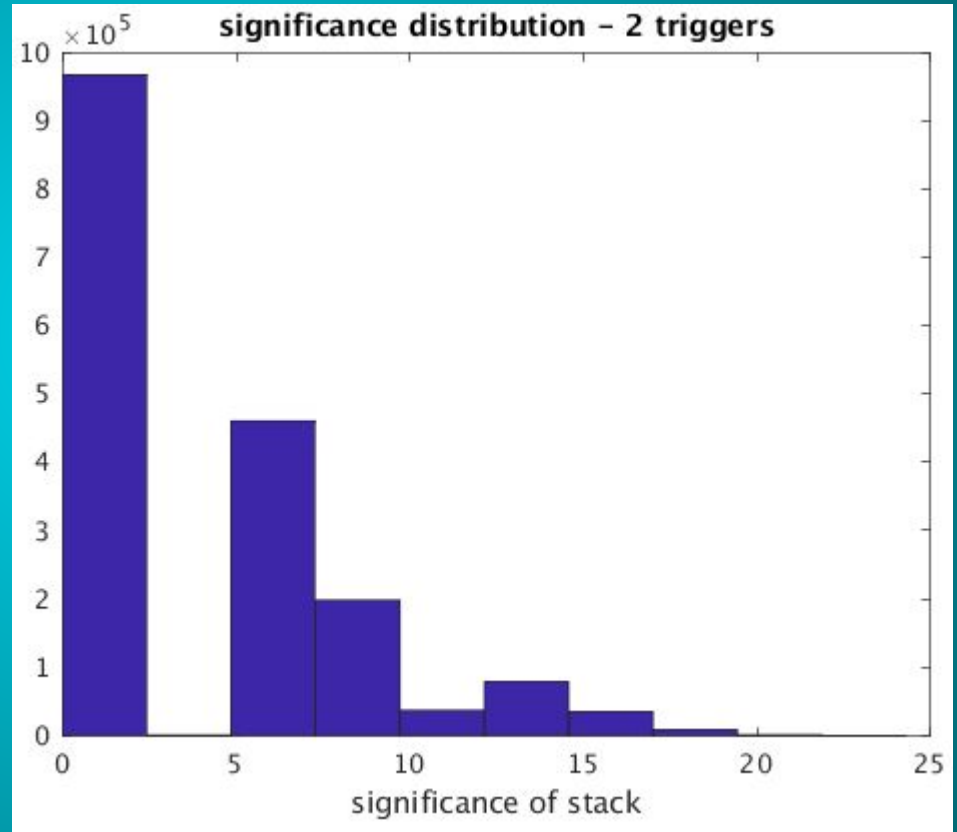
## Solution:

- We examine each frequency bin independently (each on-source frequency is compared to the off-source at that frequency).
- This will leave us with a distribution of p-values.



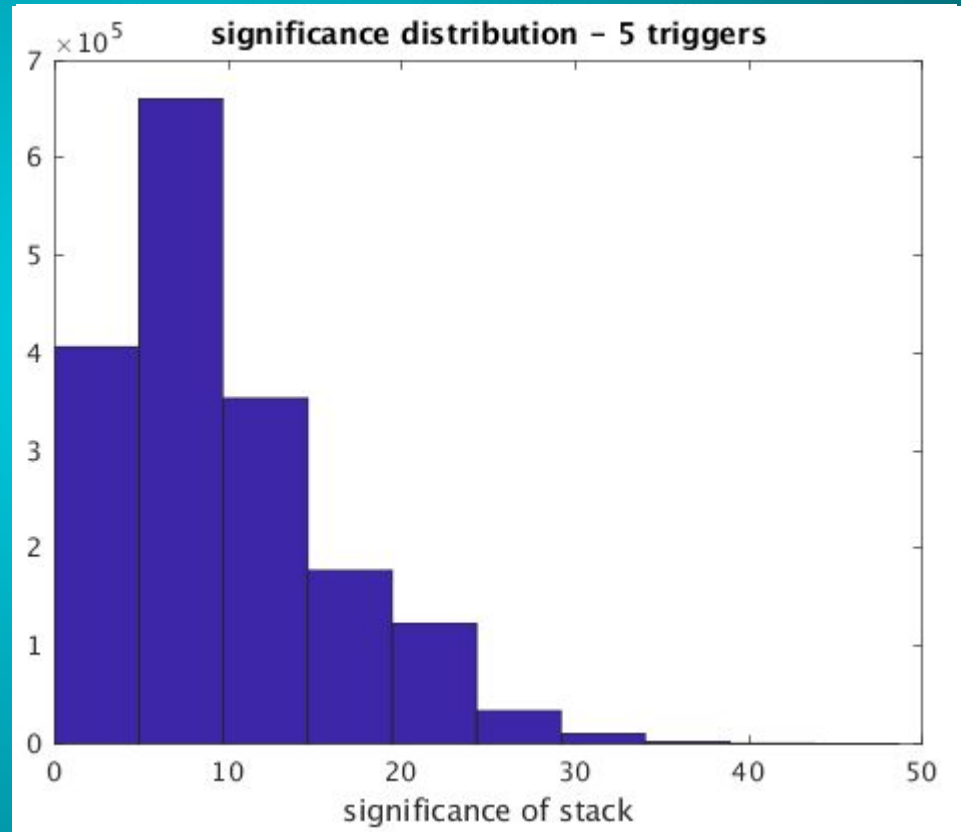
# Sensitivity studies - Stacking the O3 flares from SGR 1935+2154

- We search in 100Hz frequency-bins, specifically between 1500Hz - 1600Hz
- 5s time-bins



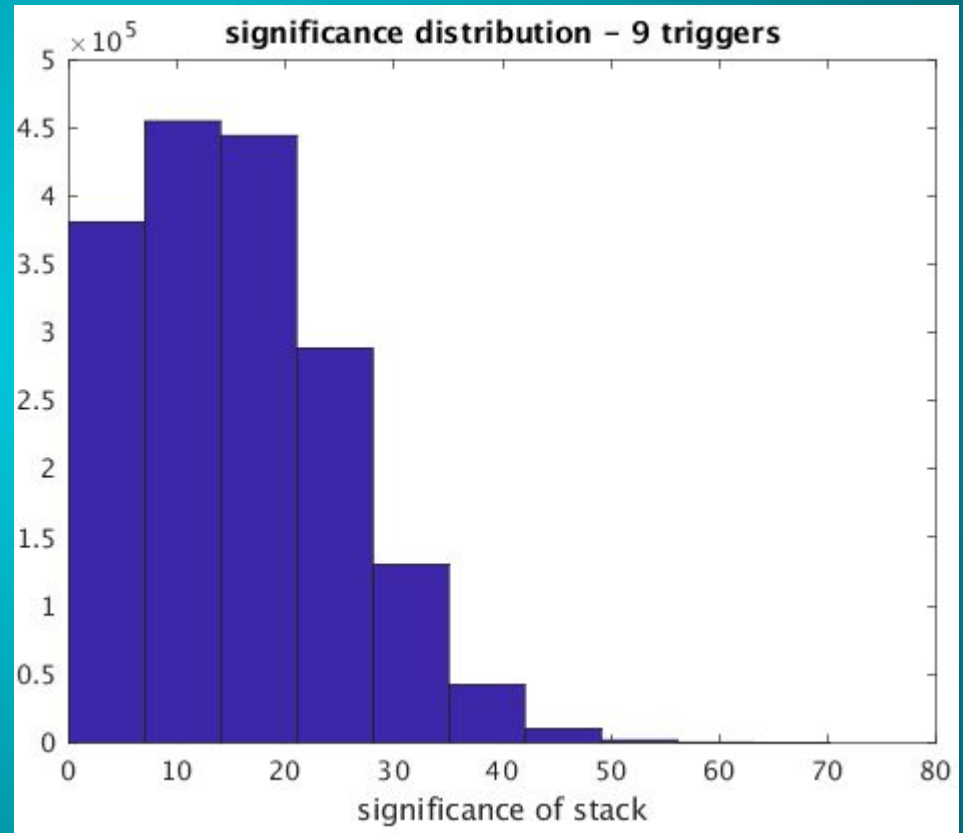
# Sensitivity studies - Stacking the O3 flares from SGR 1935+2154

- We search in 100Hz frequency-bins, specifically between 1500Hz - 1600Hz
- 5s time-bins



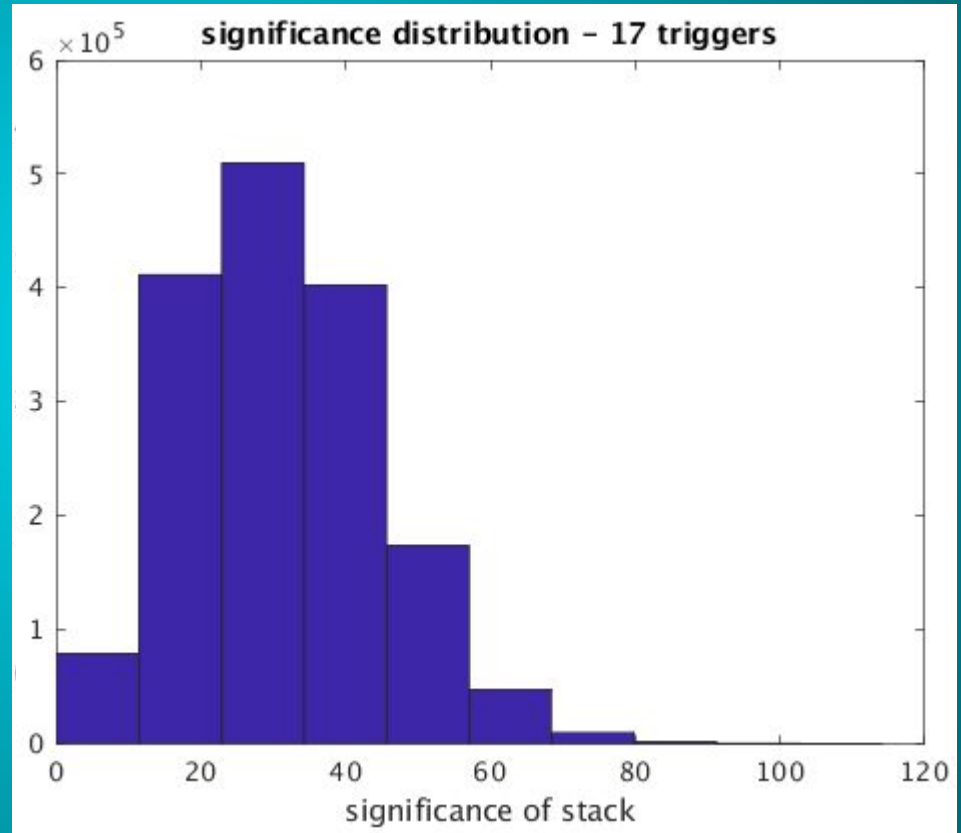
# Sensitivity studies - Stacking the O3 flares from SGR 1935+2154

- We search in 100Hz frequency-bins, specifically between 1500Hz - 1600Hz
- 5s time-bins



# Sensitivity studies - Stacking the O3 flares from SGR 1935+2154

- We search in 100Hz frequency-bins, specifically between 1500Hz - 1600Hz
- 5s time-bins

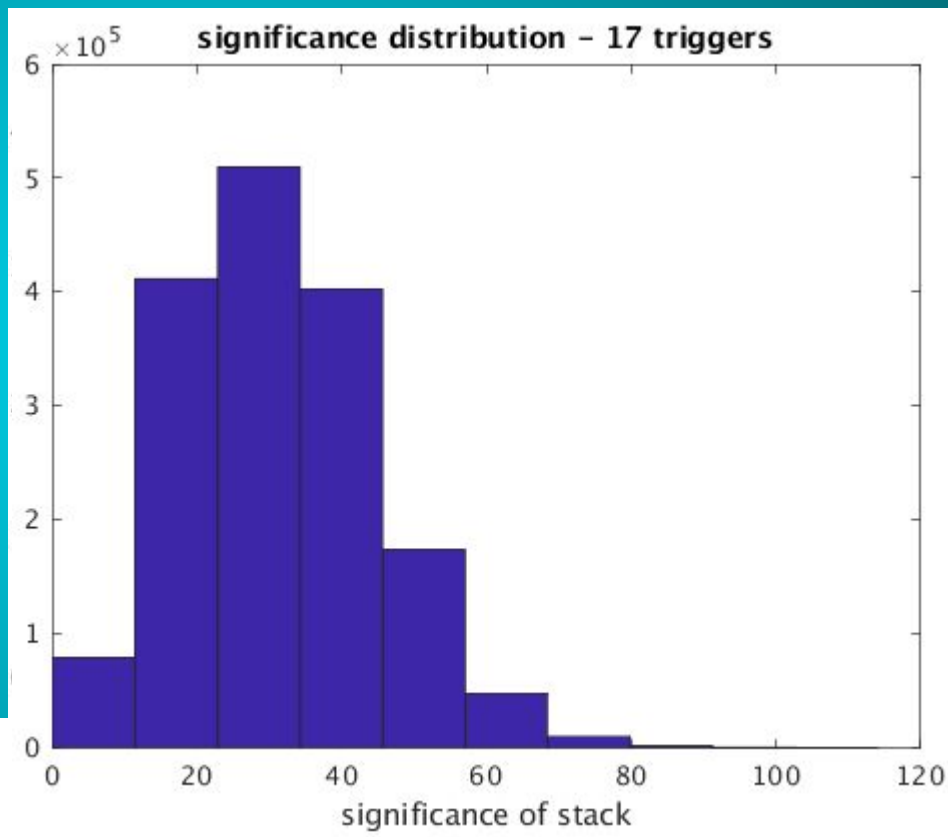




Assume that a p-value of 0.0005 constitutes an 'interesting' event.

- We can use the significance distribution of the stacked bins to estimate the threshold significance of the stack that would yield this p-value.
- Mean significance of unstacked event to give us that p-value is the threshold stacked significance/N

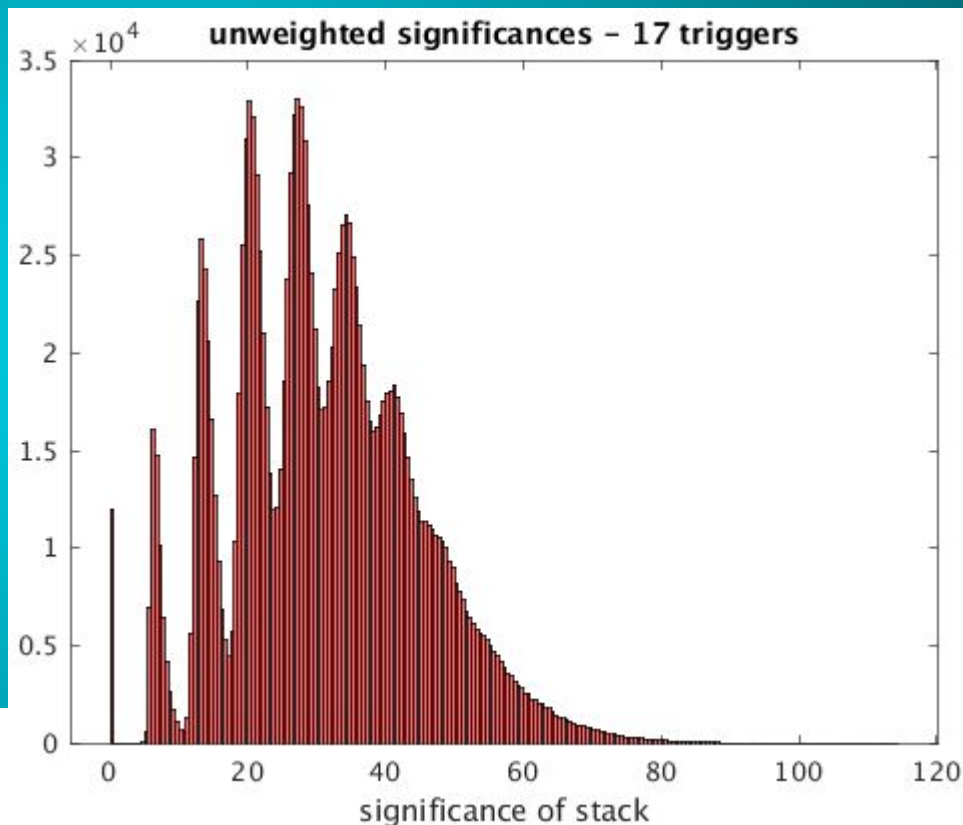
$$P = \frac{\text{Number of TF bins louder than event}}{\text{Total TF bins}}$$



Assume that a p-value of 0.0005 constitutes an 'interesting' event.

- We can use the significance distribution of the stacked bins to estimate the threshold significance of the stack that would yield this p-value.
- Mean significance of unstacked event to give us that p-value is the threshold stacked significance/N

$$P = \frac{\text{Number of TF bins louder than event}}{\text{Total TF bins}}$$

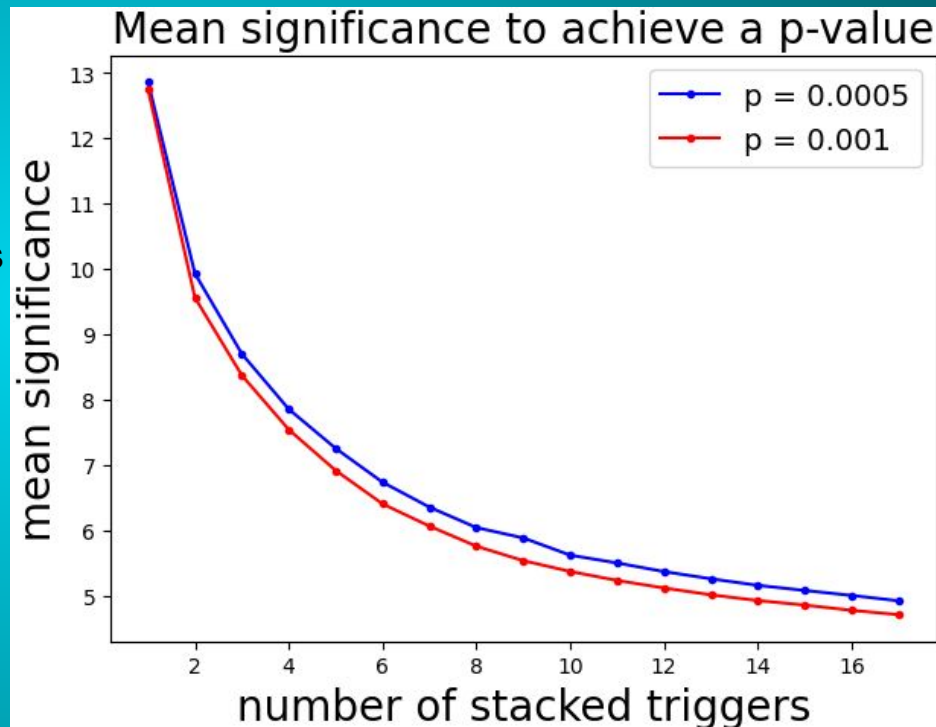


Assume that a p-value of 0.0005 constitutes an ‘interesting’ event.

We plot the mean significance needed to achieve a specific p-value, and see that we need less significance with more triggers.

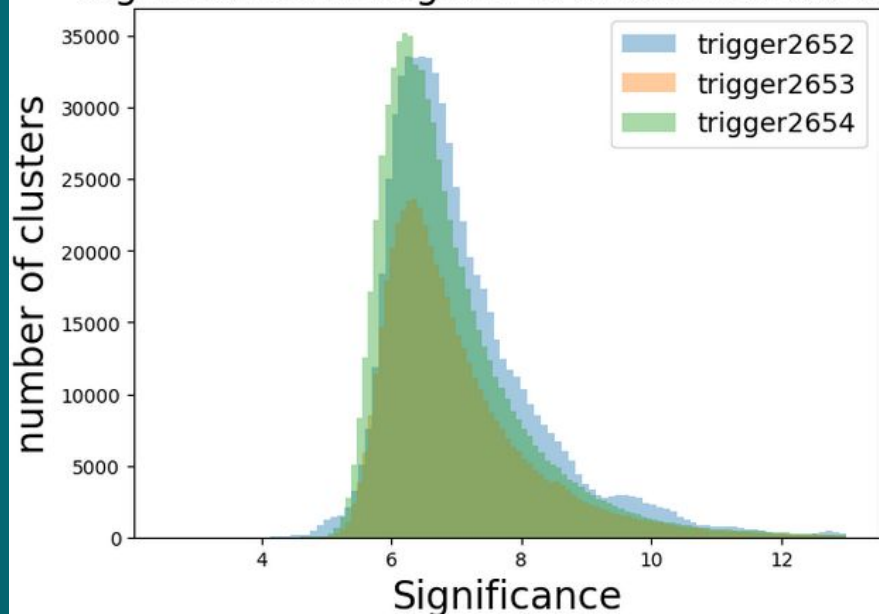
The mean significance to get a specific p-value does generally drop as we stack more triggers, and falls as low as 4.9 for 17 triggers (greatly improved from 12.9 for 1 trigger!)

Value for N=1 case is taken from the distribution of standard x-pipeline outputs, without stacking

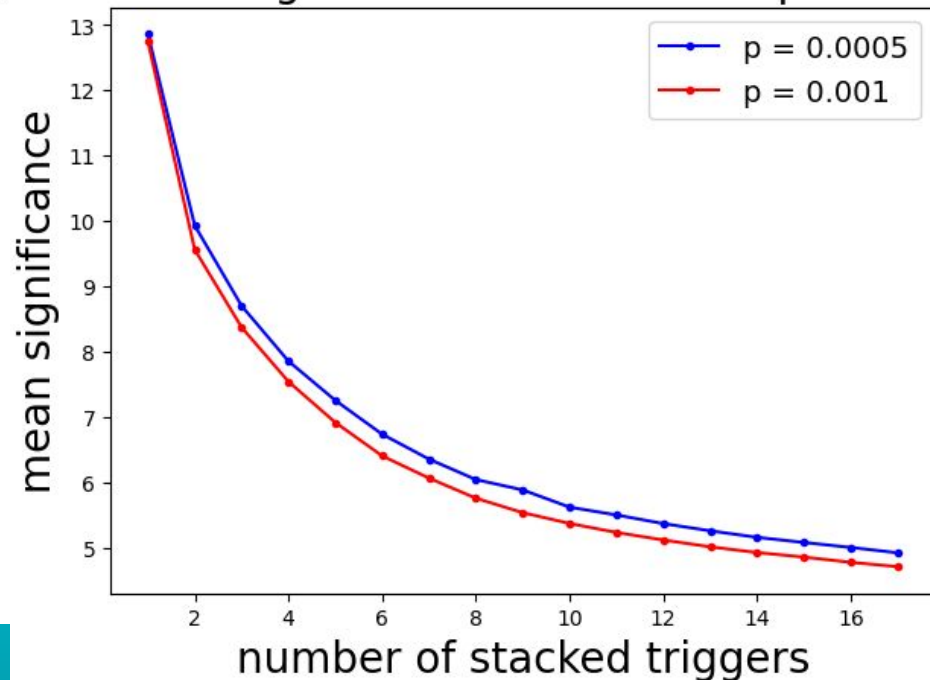


# How do these significances compare to a typical unstacked box?

Significance histogram of unstacked clusters

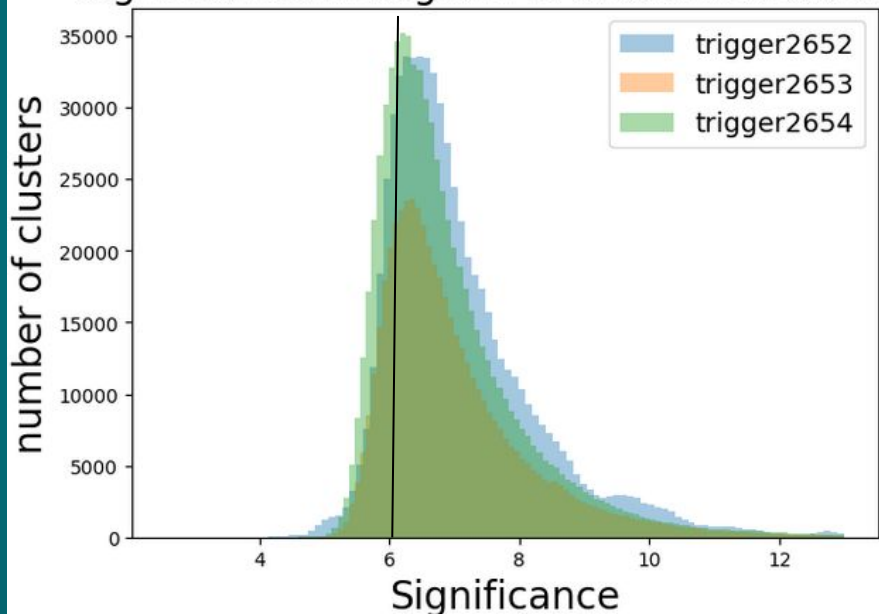


Mean significance to achieve a p-value

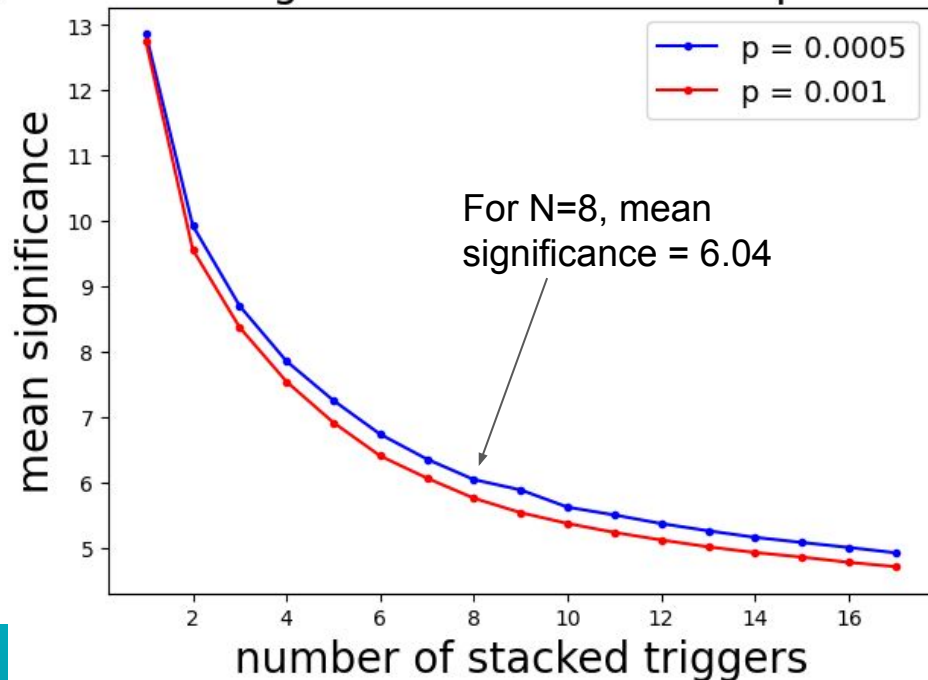


# How do these significances compare to a typical unstacked box?

Significance histogram of unstacked clusters



Mean significance to achieve a p-value



Stacking 8 triggers allows us to detect signals which would otherwise be buried in the background, as long as they are consistently present.

# Weight the significances of each trigger

(By network sensitivity now, and EM fluence later)

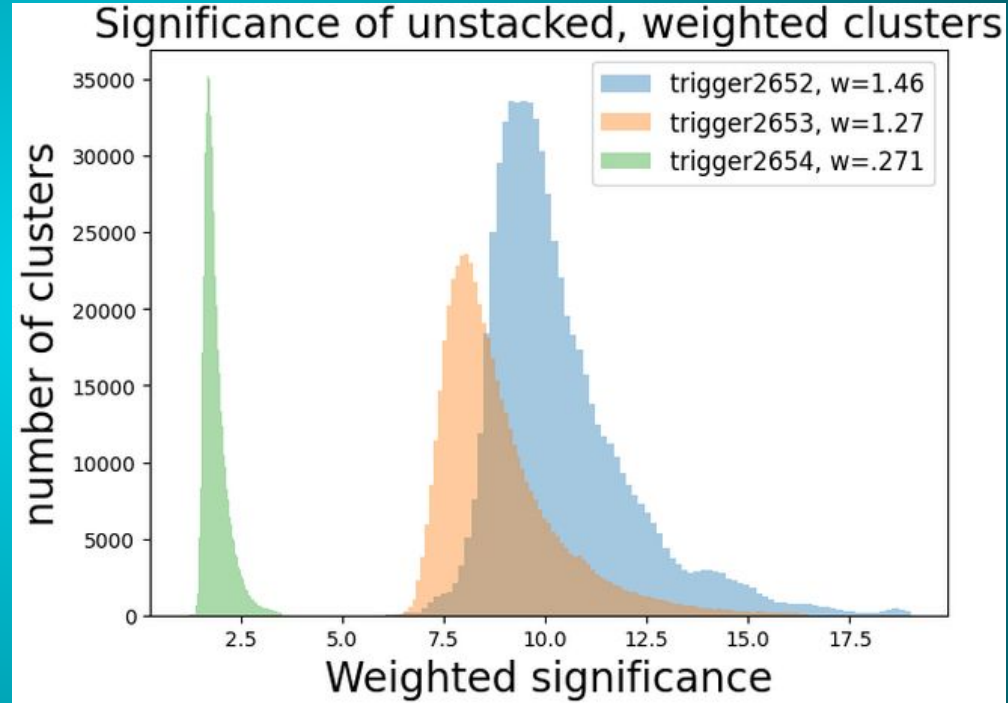
$$\text{Network Sensitivity} = \sum_{\text{Detectors}} \text{Range} \times \text{Antenna Factor}$$

$$W_{\text{box}} = \frac{\text{Network Sensitivity}}{\sum_{\text{boxes}} \text{Network Sensitivities}} \times \text{Number of Triggers}$$

We multiply the significance of each event by the weighting factor of its box. The distributions of events separate, but the mean significance across all events changes very little.

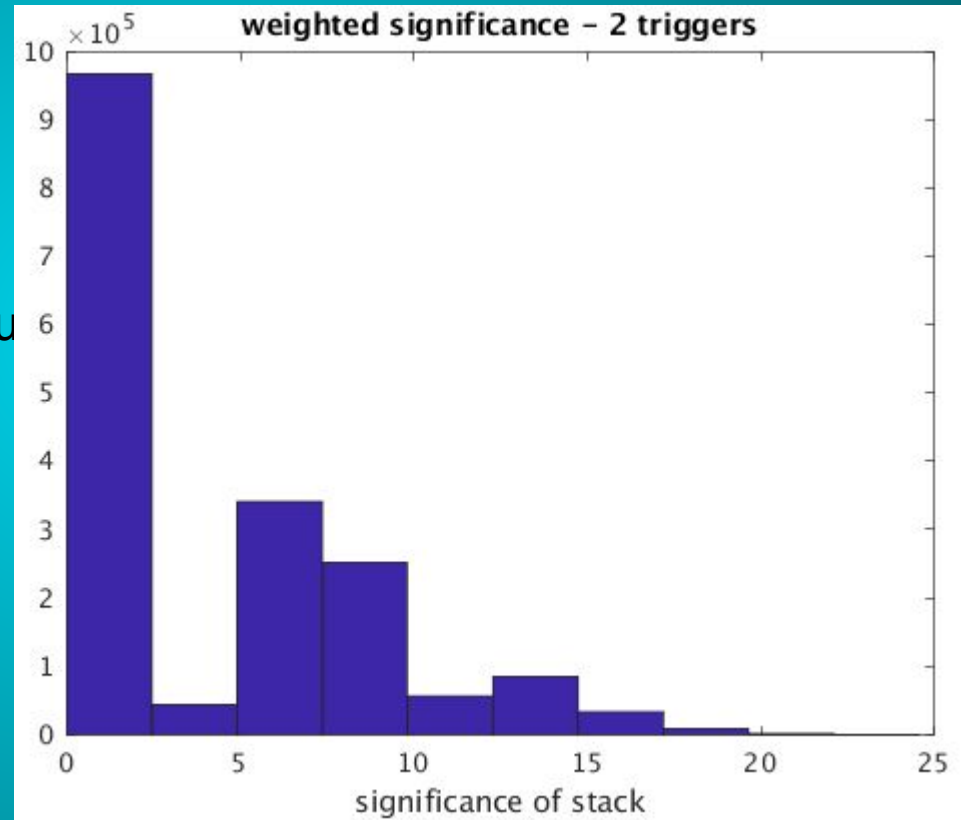
## Additional Observations:

- Trigger 2653 has fewer clusters. Less data available, and more of the clusters falling at frequencies outside this band.
- Trigger 2652 has a population of loud cluster, significance~14, that might add noise to the stacked analysis



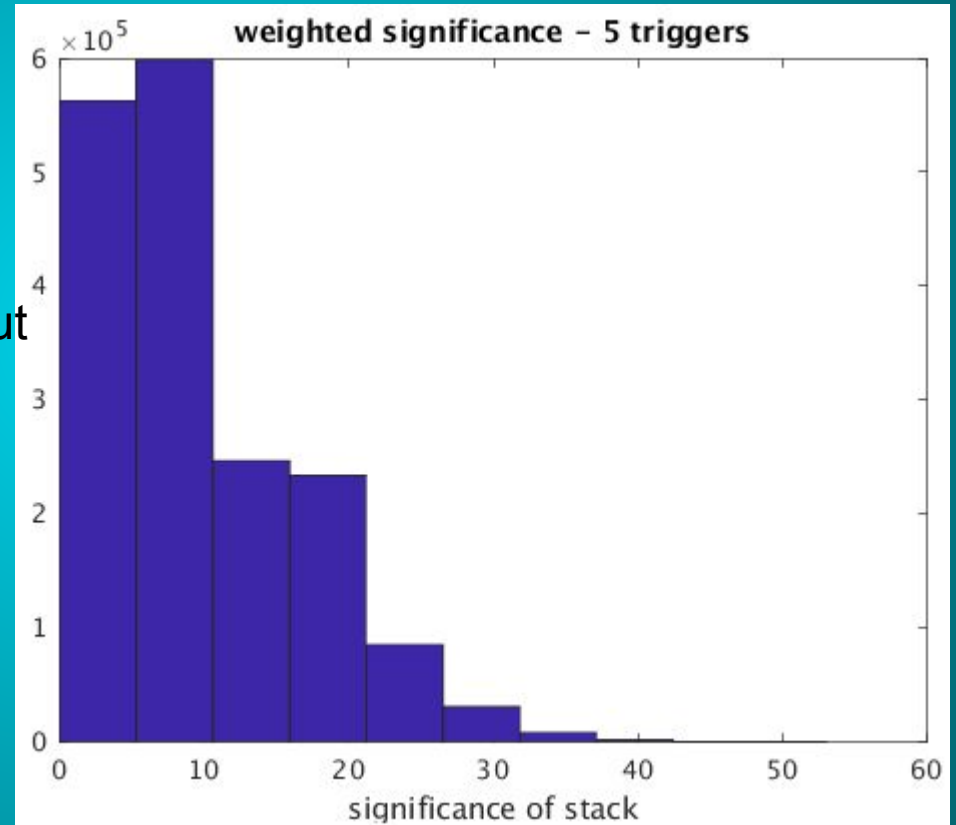
# Sensitivity Weighted Stacks - Stacking the O3 flares from SGR 1935

- We search in 100 Hz frequency-bins, specifically between 1500 Hz - 1600 Hz
- 5 s time-bins
- Same analysis as previously, but with weighted clusters



# Sensitivity Weighted Stacks - Stacking the O3 flares from SGR 1935

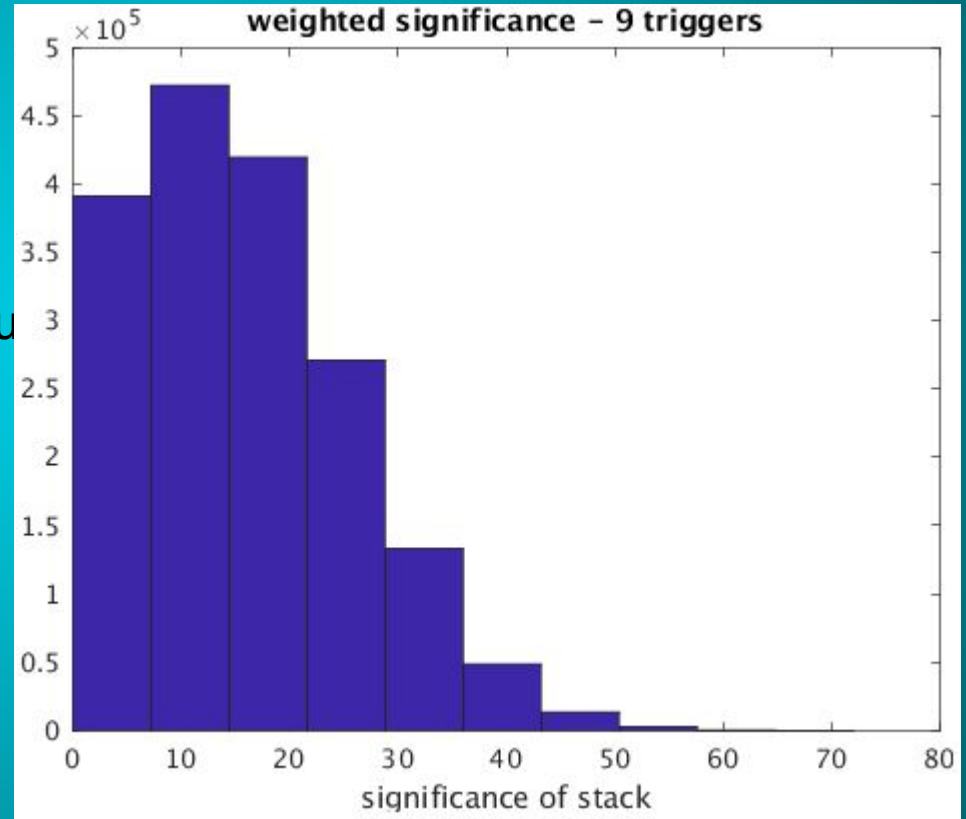
- We search in 100 Hz frequency-bins, specifically between 1500 Hz - 1600 Hz
- 5 s time-bins
- Same analysis as previously, but with weighted clusters





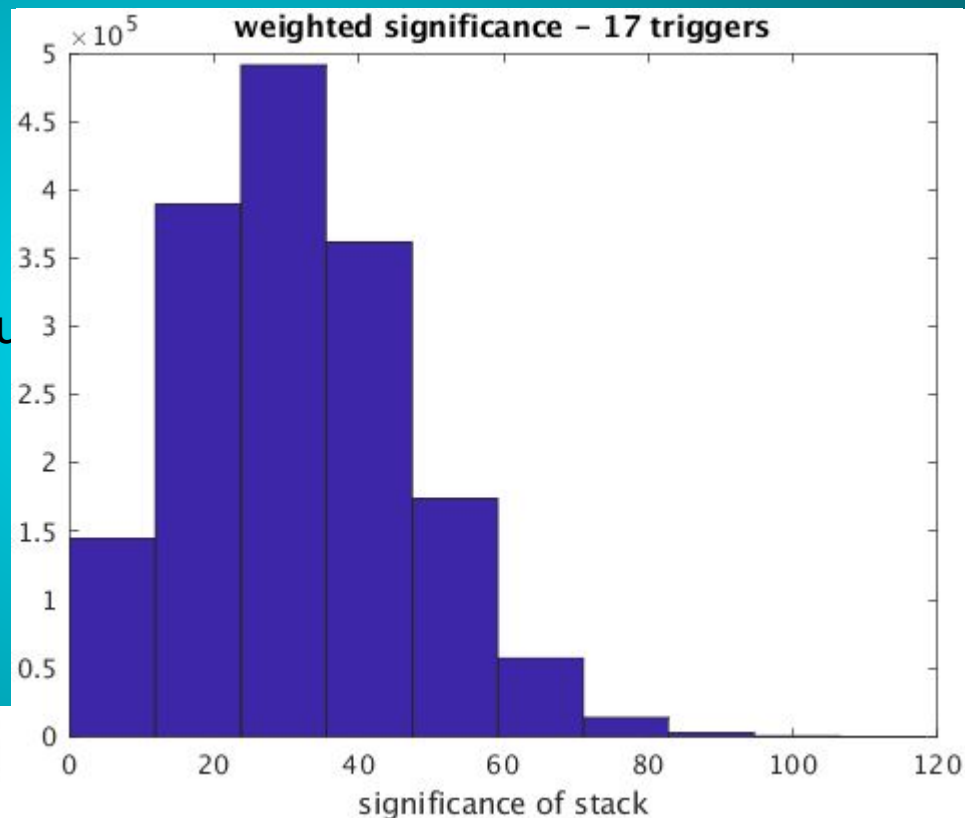
# Sensitivity Weighted Stacks - Stacking the O3 flares from SGR 1935

- We search in 100 Hz frequency-bins, specifically between 1500 Hz - 1600 Hz
- 5 s time-bins
- Same analysis as previously, but with weighted clusters



# Sensitivity Weighted Stacks - Stacking the O3 flares from SGR 1935

- We search in 100 Hz frequency-bins, specifically between 1500 Hz - 1600 Hz
- 5 s time-bins
- Same analysis as previously, but with weighted clusters

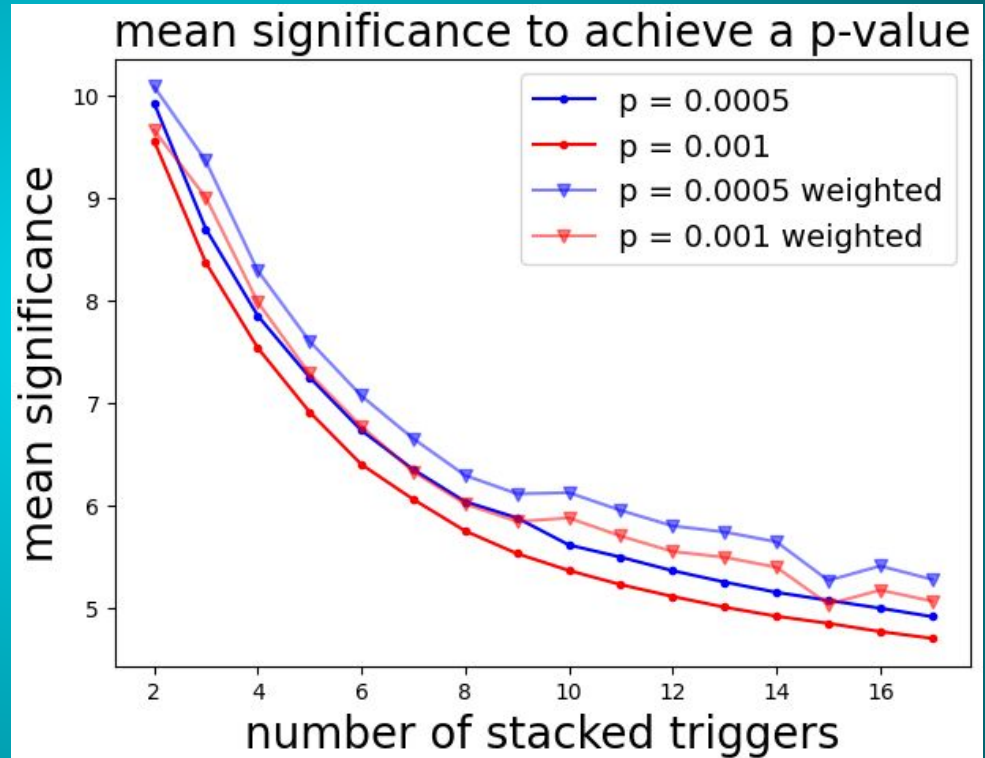


$$P = \frac{\text{Number of TF bins louder than event}}{\text{Total TF bins}}$$

# Sensitivity evolution with more stacked triggers:

We plot the weighted mean significance of the unstacked TF bins that would yield a specific p-value, given the number of triggers in each stack.

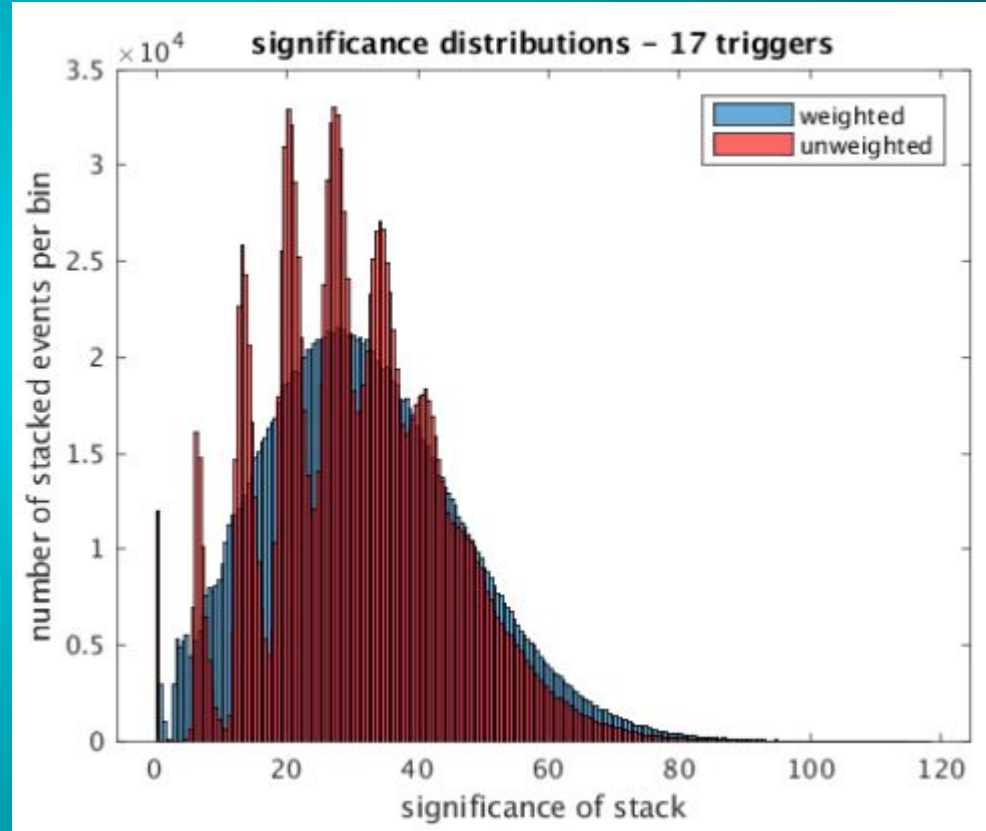
In all cases, a higher mean significance is needed when the triggers are weighted. This is consistent with the wider distribution of significances in the stacked case.



# Histograms of the stacked significance:

Histograms of the stacked significances for both the weighted (blue) and unweighted (red) cases.

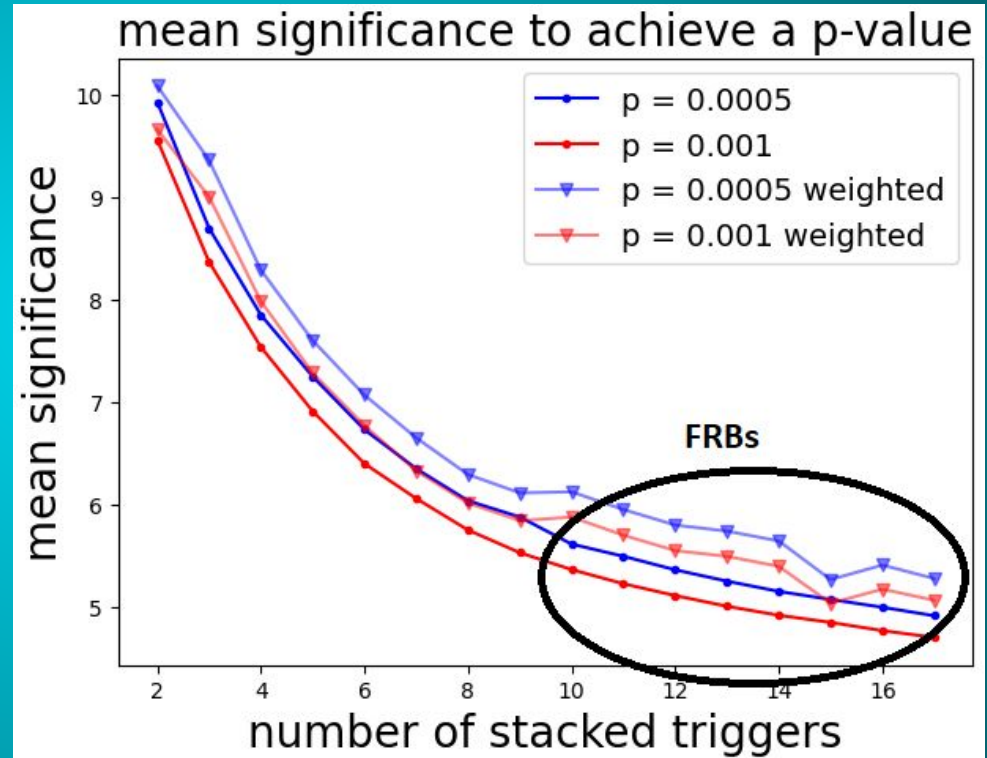
- The weighted case is wider
- The high-significance portions of these distributions the cutoff mean significance per trigger at which we can make a detection.
- Note that the periodic spikes are gone in the weighted case.



# Sensitivity evolution with more stacked triggers:

We plot the weighted mean significance of the unstacked TF bins that would yield a specific p-value, given the number of triggers in each stack.

We FRB runs we've included in this analysis were in general more sensitive than the magnetar runs. Weights spanned an entire order of magnitude.



# Reduction in hrss50% needed for a detection

We measure the hrss of injection at which 50% are recovered at a significance such that the stacked event would have a p-value =  $5 \times 10^{-4}$ .

- The hrss is decreasing with more triggers in the stack
- We use a 1590 Hz ringdown waveform with 100ms duration.
- Found using the post-processing of x-pipeline, inconsistently functional.

Number of triggers	$h_{\text{rss}}^{50\%} (\times 10^{-22} \frac{1}{\sqrt{\text{Hz}}})$	
	trigger 2655	trigger 2656
1	2.17	2.03
2	1.85	1.75
3	-	1.62
5	1.36	1.51

# Quantifying the significance reduction

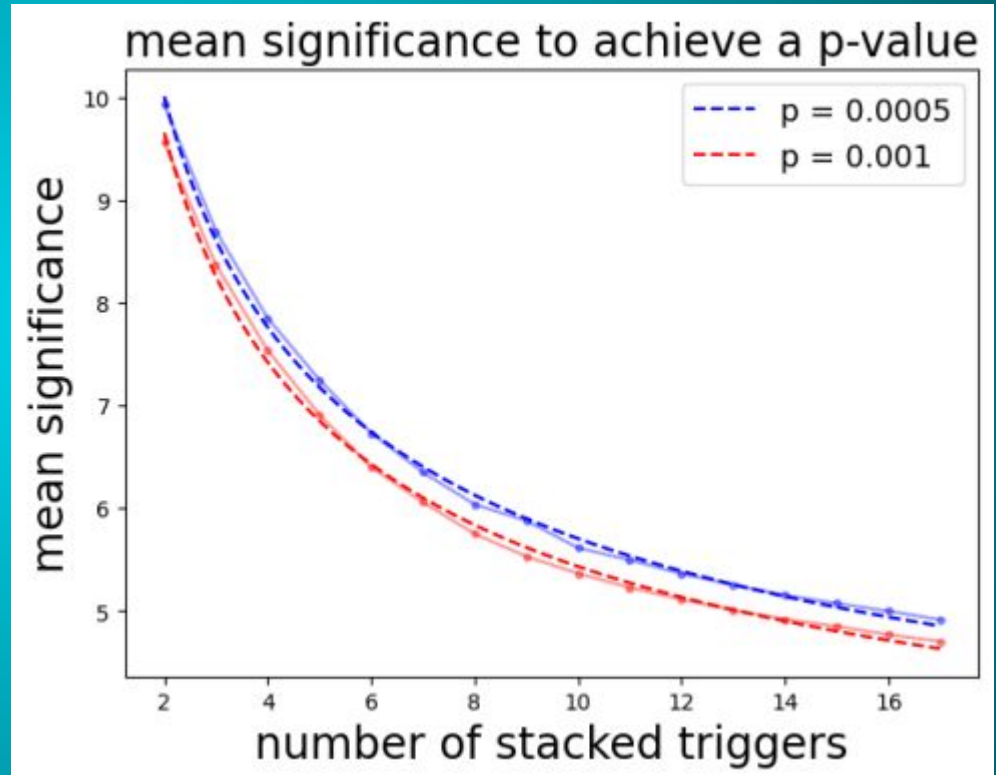
Equations of best fit (assuming a power law):

$$S_{5 \times 10^{-4}} = 1.78 + 11.32 \times N^{-0.46}$$

$$S_{1 \times 10^{-3}} = 1.97 + 10.83 \times N^{-0.49}$$

## How many triggers can we stack?

- On average, the lowest significance cluster in each box has significance of **3.19**.
- According to the above equations, we reach that with **93** triggers.



# Search parameters available to tweak

- **Time and frequency bin sizes** - these should be set by astrophysical models
- The **bright pixel percentage** - where the initial stage of x-pipeline defines a bright pixel (1% in burst searches).
- The **superdecimate rate** - the number of clusters per second that x-pipeline keeps (averaged over each block of time it analyzes). Standard is 1 cluster per 4 s.
- The **time-step dt** which x-pipeline uses for the Fast Fourier Transform to make the original time-frequency maps. Standard for an x-pipeline burst search is to use powers of  $\frac{1}{2}$  ranging from -1 to 7. We could maybe just use lower values (we expect short-duration signals).
- **Weighting** by electromagnetic fluence - this should be determined by astrophysical models.

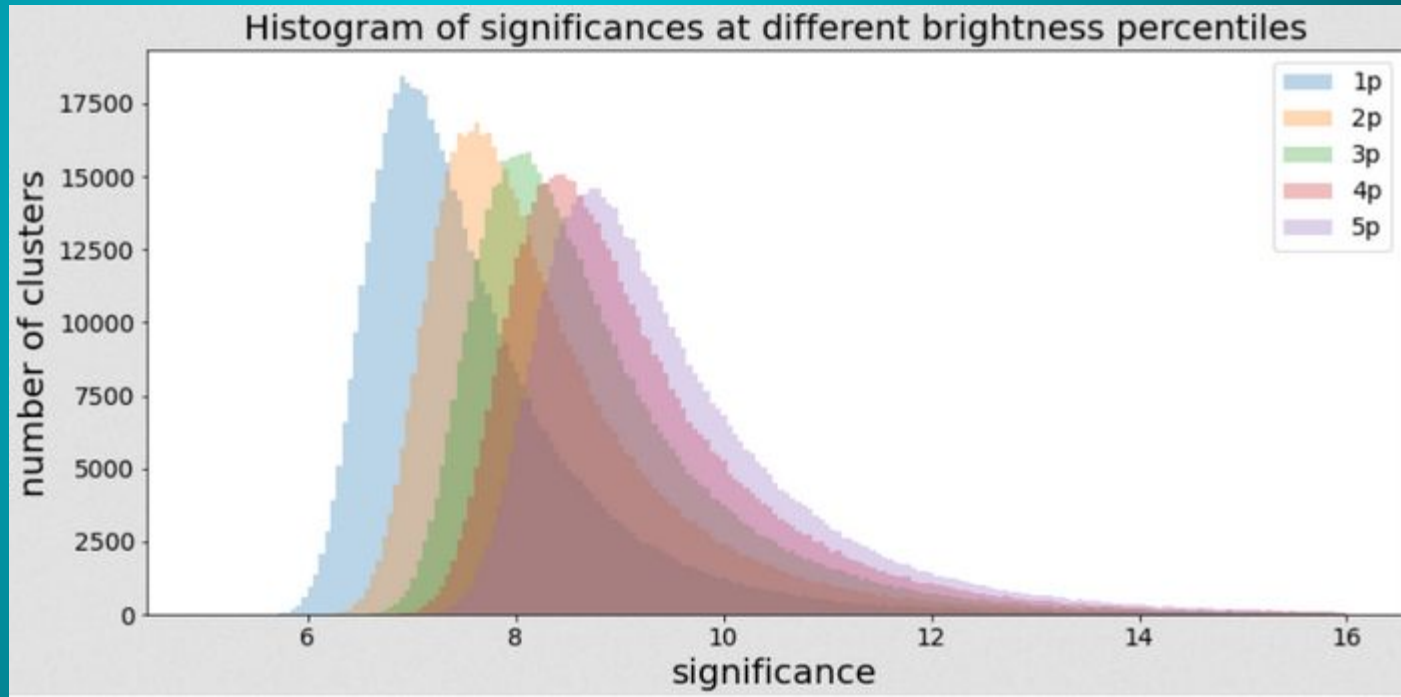


# Bright Pixel Percentage

Combined outputs of x-pipeline from triggers 2669, 2670, and 2671 run with varying bright pixel percentages.

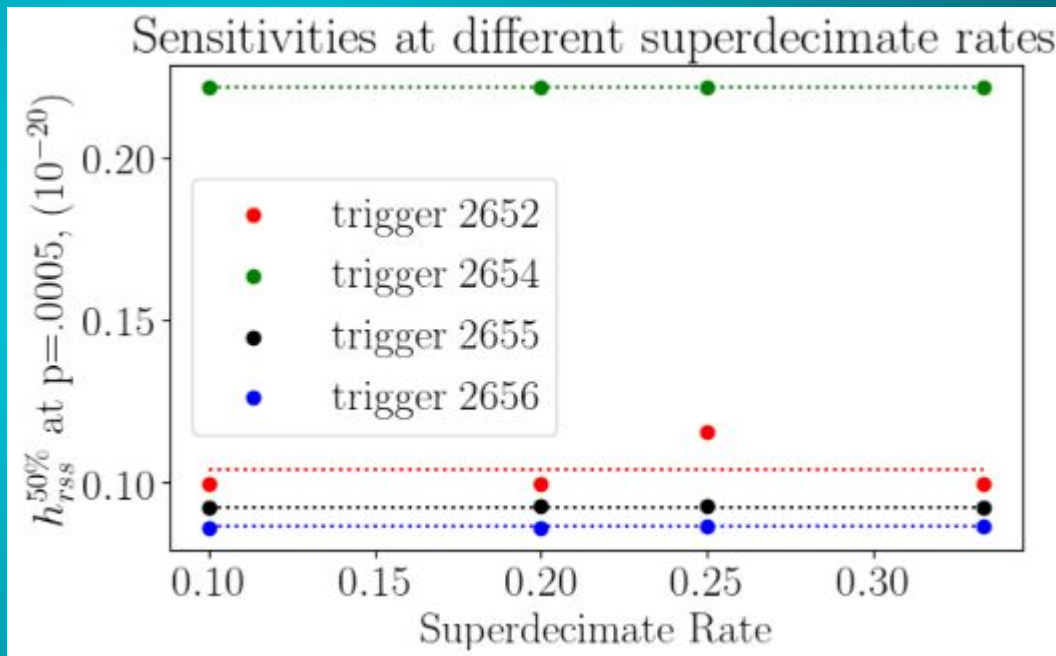
Higher bright pixel percentage means the distributions are wider.

This could raise the number of triggers that can be stacked (currently 93).



# Superdecimate Rate (clusters per second)

- Standard x-pipeline burst searches use  $\frac{1}{4}$ .
- For 3 out of the 4 x-pipeline runs, this parameter had minimal effect on the sensitivity.
- For trigger 2652, it varied by 15%



# Where is the benefit to stacking?

- Effectively **decreases the significance of an event needed to make a detection**. X-pipeline records the hrss needed to recover 50% of the injections with a greater significance than the loudest background cluster, which could be as high as **13** (our cutoff). Stacking would just require the mean significance to just be as high as the mean significances calculated on the previous slide, (as low as **4.9**).
- This analysis is run on magnetar flares which have already been analysed individually using X and not shown evidence of a GW. So this is a way to look for lower-significance GWs.

# Stacking Summary:

- This method could obtain a **p-value as low as  $6.7 \times 10^{-7}$**
- The mean significance necessary to achieve a p-value of .0005 can get as low as **4.9 with 17 stacked triggers.**
- We already have sources to run and evaluate this on including 9 flares from SGR 1935+2154, 2 from Swift J1818-1607, the 3 bursts from the unknown magnetar.
- We've run X-pipeline on repeating FRBs as well, if we have one with many repeats this could be interesting.
- We could have more sources and interesting events in O4 and beyond.

# Publications

56 LIGO Scientific Collaboration papers published between 2018 and the present.

Publications for which I was on the paper-writing team:

The LIGO Scientific Collaboration, the Virgo Collaboration, the KAGRA Collaboration, and CHIME/FRB Collaboration. Search for gravitational waves associated with fast radio bursts detected by chime/frb during the ligo-virgo observing run o3a. 2022. Submitted to the *Astrophysical Journal*.

Publications for which I was a co-manager:

The LIGO-Virgo-KAGRA Collaboration. Search for gravitational-wave transients associated with magnetar bursts in advanced ligo and advanced virgo data from the third observing run, 2022. URL <https://arxiv.org/abs/2210.10931>. Submitted to the *Astrophysical Journal*.

Publications for which I participated as a data analyst:

The LIGO-Virgo-KAGRA Collaboration. Search for gravitational waves associated with gamma-ray bursts detected by fermi and swift during the LIGO-virgo run o3a. *The Astrophysical Journal*, 915(2):86, jul 2021. doi: 10.3847/1538-4357/abee15.

The LIGO-Virgo-KAGRA Collaboration. Search for gravitational waves associated with gamma-ray bursts detected by fermi and swift during the LIGO-virgo run o3b. *The Astrophysical Journal*, 928(2):186, apr 2022. doi: 10.3847/1538-4357/ac532b.

Conference Preceedings:

Kara Merfeld. Search for gravitational-wave transients associated with magnetar bursts during the third advanced LIGO and advanced virgo observing run. *Proceedings of the International Astronomical Union*, 16(S363): 187–190, Jun 2020. doi: 10.1017/s1743921322002629. URL <https://doi.org/10.10172Fs1743921322002629>.

Instrumental author list publications:

D. Davis et al. LIGO detector characterization in the second and third observing runs. *Classical and Quantum Gravity*, 38(13):135014, jun 2021. doi: 10.1088/1361-6382/abfd85. URL <https://doi.org/10.10882F1361-63822Fabfd85>.

S Soni et al. Reducing scattered light in LIGO's third observing run. *Classical and Quantum Gravity*, 38(2):025016, jan 2021. doi: 10.1088/1361-6382/abc906. URL <https://doi.org/10.10882F1361-63822Fabc906>.

A. Buikema et al. Sensitivity and performance of the advanced LIGO detectors in the third observing run. *Physical Review D*, 102(6), sep 2020. doi: 10.1103/physrevd.102.062003. URL <https://doi.org/10.11032Fphysrevd.102.062003>.

# Acknowledgements

I would like to acknowledge my family and friends who have supported me throughout my graduate school career, and my collaborators for their insightful ideas and research help.

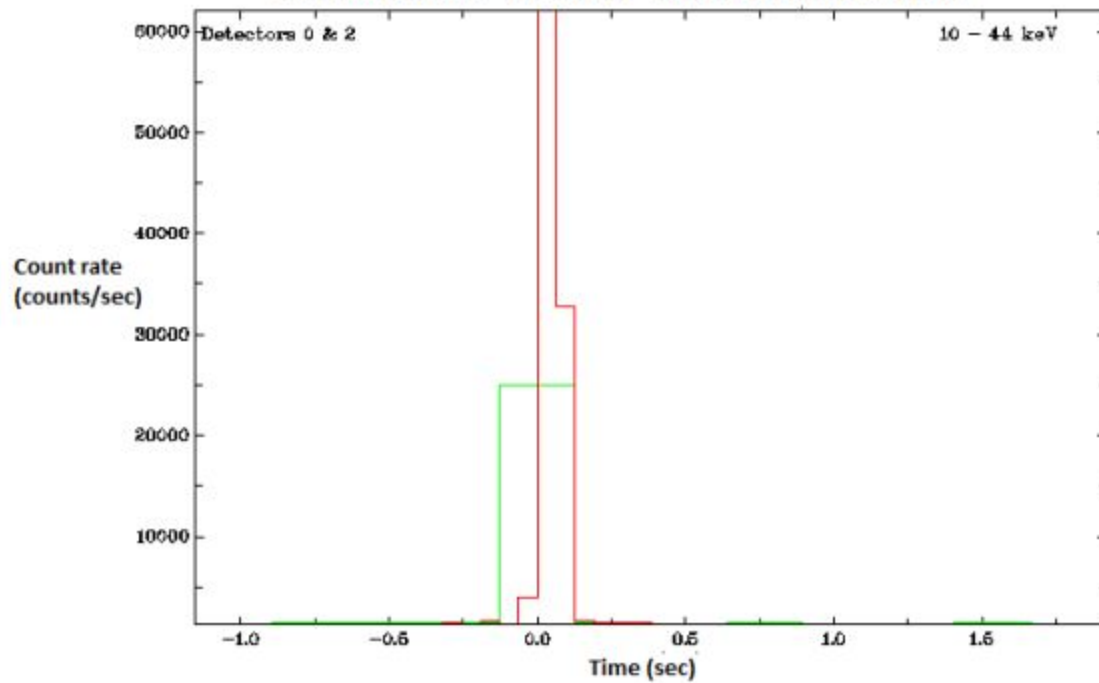
I also would like to thank the essential workers for their service during the pandemic, which allowed the rest of us to continue working from home.

I also owe my gratitude to the people I met on my travels who hosted me and welcomed me into their communities in Ireland, NI, Mozambique, Tanzania, Egypt, France, Scotland, Portugal and Greece.



# Extra Slides

GLAST Burst Monitor - Trigger 2656 - Nov. 4th, 2019, 10:44:26.31 UTC





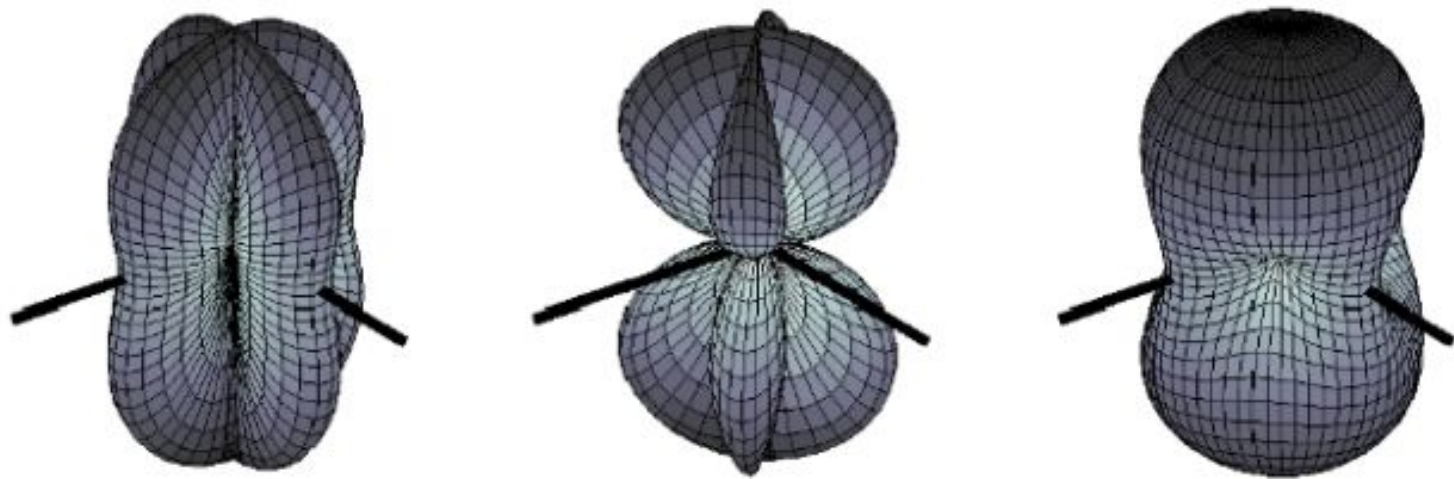


FIGURE 5. Antenna response pattern for a gravitational wave detector for the + polarization (left), the X polarization (center) and mean polarization (right) [6, 7]. The arms of the gravitational-wave detector are taken to lie along the black lines, and the radius from a point on the surface to the origin represents the sensitivity to gravitational waves of that polarization in that direction.